EUROPEAN CENTRAL BANK
EUROSYSTEM

Working Paper Series

Danilo Leiva-Leon, Gabriel Perez-Quiros, Eyno Rots

Real-time weakness of the global economy: a first assessment of the coronavirus crisis

No 2381 / March 2020

Abstract

We propose an empirical framework to measure the degree of weakness of the global economy in real-time. It relies on nonlinear factor models designed to infer recessionary episodes of heterogeneous deepness, and fitted to the largest advanced economies (U.S., Euro Area, Japan, U.K., Canada and Australia) and emerging markets (China, India, Russia, Brazil, Mexico and South Africa). Based on such inferences, we construct a Global Weakness Index that has three main features. First, it can be updated as soon as new regional data is released, as we show by measuring the economic effects of coronavirus. Second, it provides a consistent narrative of the main regional contributors of world economy's weakness. Third, it allows to perform robust risk assessments based on the probability that the level of global weakness would exceed a certain threshold of interest in every period of time.

Keywords: International, Business Cycles, Factor Model, Nonlinear.

JEL Classification Code: E32, C22, E27.

Non-technical summary

We propose an empirical framework to measure the degree of weakness of the global economy in real-time. It relies on nonlinear factor models designed to infer recessionary episodes of heterogeneous deepness, capturing the intuition that recession periods are different from each other. Incorporating this feature allow us to improve the fit of the model and the dynamics of expansion and recession periods. We estimate the model using data from the largest advanced economies (U.S., Euro Area, Japan, U.K., Canada and Australia) and emerging markets (China, India, Russia, Brazil, Mexico and South Africa). Based on such inferences, we construct a Global Weakness Index that has three main features. First, it can be updated as soon as new regional data is released, as we show by measuring the economic effects of coronavirus. Second, it provides a consistent narrative of the main regional contributors of world economy's weakness. Third, it allows to perform robust risk assessments based on the probability that the level of global weakness would exceed a certain threshold of interest in every period of time. With this specification, we show that after the release of the soft indicators on March 2nd 2020 the Global Weakness Index has sharply increased at a speed at least comparable to the experienced in the 2008 crisis.

1 Introduction

The last Global Financial Crisis has had ramifications that, arguably, can be seen to this day across the globe. Europe has been no exception: it has witnessed a dramatic recession in 2008–2009 across the euro area and the Sovereign Debt Crisis in 2009–2012; ever since, it has been plagued by lacklustre growth that has turned resistant to a plethora of unprecedented non-conventional monetary and fiscal stimuli. More recently, there has been growing concern among academics and policy-makers about a new recessionary phase. This concern is not confined to U.S. and the Euro Area. Based on the latest adverse global economic developments, influenced by the outbreak of a new disease in China associated to a new coronavirus, and spread around the globe, international organizations, such as the IMF and the OECD, have downgraded to outlook of the world economy.[1] Given the looming danger of a new global downturn, the need for a framework to infer the strength of the world economy in real-time is as high as ever.

Given two of the main defining characteristics of business cycles, which are comovement across real activity indicators and nonlinear dynamics resembling up and downturns (Burns and Mitchell (1946)), previous works have proposed econometric frameworks that account for these features when inferring recessionary episodes. In particular, Markov-switching dynamic factor (MSDF) models have been successfully used to account for comovements and nonlinearities in a unified setting. Introduced by Chauvet (1998), MSDF models where initially applied to a set of U.S. real activity indicators at the monthly frequency with the aim of summarizing such information into a single index subject to regime changes, showing its ability to identify turning points in a timely fashion.[2] Other works have focused on extending such a framework to operate in the context of mixed-frequency data, to include information on quarterly real GDP (Camacho et al. (2014)) or on nominal GDP (Barnett et al. (2016)).

In the context of MSDF models, the common factor summarizing the information in a set of activity indicators is assumed to have an unconditional mean associated to expansions, μ_{exp}, and another unconditional mean associated to recessions, μ_{rec}. Following Hamilton (1989), previous MSDF models have assumed that μ_{exp} holds for all the expansions, and that μ_{rec} also holds for all recessionary episodes, included in the sample. However, this assumption can be highly restrictive, in particular, if recessions are considerably heterogeneous over time in terms

[1] In February 22nd 2020 the IMF decreased 0.1% global growth, IMF (2020). Only a week later, on March 2nd the OECD decreased global growth in 0.5%, OECD (2020).

[2] Chauvet and Piger (2008) rely on a similar model, however, it is estimated with Bayesian instead of classical methods.

of deepness. For example, assuming that μ_{rec} does not vary across recessions could preclude the model to accurately infer an upcoming 'mild' recession after having only observed a 'severe' recession, as happened in most advanced economies after the Global Financial Crisis. Hence, although MSDF models allow for a timely assessment of turning points by relying on a set of indicators, they might be subject to a lack of accuracy when implemented in a context of heterogeneous downturns, which is typically observed at the international level. Jerzmanowski (2006) shows that output growth of emerging economies exhibit substantially different types of recurrent recessionary regimes. Also, Aguiar and Gopinath (2007) illustrate that modelling business cycles nonlinearities associated to emerging markets tends to be even more challenging than for the case of developed economies.

In a more recent work, Eo and Kim (2016) propose a model that uses real GDP growth data to produce inferences of U.S. recessions by taking into account their heterogeneity over time. The model consists of a univariate Markov-switching specification subject to time-varying means (MSTM). In particular, the authors assume that quarterly GDP growth has an unconditional mean μ_{exp,τ_0}, associated to the τ_0-th expansion, and an unconditional mean μ_{rec,τ_1}, associated to the τ_1-th recession, in the sample under consideration. That is, each expansionary and recessionary episode has its own corresponding unconditional mean. While this feature certainly helps to accurately detect turning points in a context of heterogeneous downturns, this model only produces inferences for one low frequency variable, quarterly GDP growth. Such a feature precludes the MSTM model delivering a robust assessment on the state of the economy, based on a set of activity indicators, that can be updated in real-time, which is of high relevance due to the rapidly changing economic environment.

The aim of this paper is developing a flexible empirical framework, that accounts for downturns of heterogeneous deepness and that also can be used in a real-time environment, to provide robust assessments on the strength of the global economy. Such assessments are based on information gathered from the largest world's economies, both advanced and emerging. In doing so, we proceed in two steps. First, we design a nonlinear factor model that allows for mixed frequency data and time-varying recession means, that is, we combine the multivariate setting associated to the MSDF model with the nonlinearities embedded in the MSTM model. By using data on economic indicators at the monthly and quarterly frequency, the model is independently fitted to six advanced economies and six emerging markets. The selection of the countries is based on the size of their economies, covering altogether more than seventy percent of the world

GDP.[3] Due to its flexibility in dealing with nonlinearities, our model is able to reproduce, for all the regions, timely and accurate inferences on regimes of weak activity, which are aligned with corresponding downturns in output growth. Second, the inferences associated to the twelve regions are summarized into a single Global Weakness Index (henceforth GWI) that assesses the state of the world economy, and that can be updated on a daily basis, whenever new information on the regions is released. To the best of our knowledge, this is the first model-based index that uses economic data to provide updates on the state of the global economy with such a high frequency.[4]

An important feature of the GWI is that is bounded between zero and one, where values close to one represent high weakness and values close to zero indicate low weakness. This feature facilitates its interpretation and also comparisons between different episodes of interest. We show that the proposed index timely tracks periods where the global economy has been substantially weak, such as the period of the Great Recession, between the late 2015 and early 2016, and the present time. Also, we compare the ability of our framework with non-model-based measures of the state of the world economy, finding that the GWI largely leads the perception of agents about an upcoming global recession, proxied by information based on web searches.

Since the weakness at the global level is based on a weighted average of the weakness at the regional level, the GWI can be straightforwardly decomposed into the time-varying contributions associated to each region. Based on this decomposition, we provide a narrative of the evolving strength of the global economy and its main contributors. In particular, we quantify the substantial importance of U.S., by the end of 2007, in the deterioration of global economic conditions, and the large influence that had emerging markets on the global recovery phase, in the late 2009. Lastly, the GWI is employed to monitor global risks in real-time. This is carried out by computing the probability that the level of global weakness would exceed a certain threshold of interest. This information is collected in a real-time environment, providing the entire spectrum of risks associated to a downturn of the world economy.

Finally, when the paper was almost written, unexpected and adverse global economic development took place. In January 2020 an outbreak of a new disease associated with the coronavirus (COVID-19) hitted the international stock markets and trade activity. Motivated by

[3]For advanced economies, we include U.S., Euro Area, Japan, U.K., Canada and Australia, and for emerging markets, China, India, Russia, Brazil, Mexico and South Africa.

[4]On a related work, in a linear framework, Kilian (2019) relies on information on shipping costs to proxy world economic activity. Although, Hamilton (2019) concludes that data on world industrial production provides a better indication of global activity.

these events, we test the ability of the proposed methodology to detect global weaknesses in real time by assesing the effect of the coronavirus outbreak on the global economy.

The paper is organized as follows. Section 2 proposes the empirical framework to infer recessions of heterogeneous deepness. Section 3 provides inferences about the weakness of the largest world economies under consideration. Section 4 introduces the global weakness index and illustrates its main features. Section 5 concludes.

2 Inferring Heterogeneous Recessions

In this section, we introduce a new class of dynamic factor models, in which the common factor follows Markov-switching dynamics that are subject to time-varying means. The proposed model summarizes the information contained in a set of real activity indicators into a common factor that accounts for heterogeneous recessions, and that can be interpreted as an index that proxies the business cycle dynamics of a given economy. For convenience of exposition, we first focus on describing the dynamics of the latent common factor, and then, we proceed to detail how such a latent factor is extracted from the observed data.

We assume that the common factor, f_t, follows nonlinear dynamics that are flexible enough to accommodate the realization of recessions of different magnitudes,

$$f_t = \mu_0(1 - s_t) + \mu_1 s_t + s_t x_t + e_{f,t}, \quad e_{f,t} \sim \mathcal{N}(0, \sigma_f^2) \text{ i.i.d.}, \tag{1}$$

where $s_t \in \{0, 1\}$ is a latent discrete variable that equals 0 when the economy is in a 'normal' episode, and takes the value of 1 when the economy faces an 'abnormal' episode. The variable s_t is assumed to follow a two-state Markov chain defined by transition probabilities:

$$\Pr(s_t = j | s_{t-1} = i, s_{t-2} = h, ...) = \Pr(s_t = j | s_{t-1} = i) = p_{ij}. \tag{2}$$

Notice that since there are two states, these probabilities can be summarized by the chance of remaining in a normal state, p, and the chance of remaining in an abnormal state, q.

The variable x_t in Equation (1) is defined as another unobserved process that evolves over time as follows:

$$x_t = s_t x_{t-1} + (1 - s_t)v_t, \quad v_t \sim \mathcal{N}(0, \sigma_v^2) \text{ i.i.d.} \tag{3}$$

This law of motion implies that during normal times, when $s_t = 0$, x_t is a white noise which has no impact on the common factor f_t. However, during an abnormal episode, when $s_t = 1$, the value of x_t remains fixed and is passed to the common factor. Hence, the common factor has the same constant mean μ_0 in normal times, but each abnormal episode is unique in the sense that the common factor during such episode would have a mean μ_1 adjusted by the value of x_t, which, in turn, is unique for each episode. Obviously, this value x_t is calculated from the observed data, that determine the magnitud that better fit each recession period.

The novelty of the proposed nonlinear factor model is in the dynamics of the common factor, which in our case is a function of a random variable that fluctuates around a state-dependent mean to account for heterogeneous recessions. The mean of the common factor is at the same constant level in each period when the economy is in the normal state. However, when the economy switches to an abnormal state, the prior mean is drawn from a random distribution, learns from the data, and remains the same for the entire duration of the abnormal episode, until the economy reverts back to a normal episode. In other words, all normal episodes come with the same mean of the common factor, whereas each abnormal episode comes with its own unique common-factor mean.

The proposed specification falls between that of Hamilton (1989), in which the common-factor means associated to normal and abnormal episodes are two constant values, and that of Eo and Kim (2016), in which the two means are separate random-walk processes, which gradually evolve over time, allowing for different observed growth rates in times of both normal and abnormal episodes. We justify our modelling choice as the minimal specification that is necessary to account for the obvious fact that recessionary episodes come with very different growth rates of the GDP, and other real activity indicators. On the one hand, the Global Financial Crisis of 2007–2008 was unusually severe for many economies that, compared to it, subsequent recessions look barely distinguishable from normal times. For example, based on the data for many European countries, one would almost certainly fail to detect any other recession but the one observed upon the Global Financial Crisis when using a Markov-switching model with the common factor of the Hamilton type. On the other hand, for many countries, there are so few recessionary episodes observed in the available data that a rich model that allows for independent recession- and expansion-specific common factor means of the Eo-Kim type would often be challenging to estimate without large model uncertainty. The model that we propose has a minimalistic structure due to potential lack of available data for the economies of interest,

yet it is rich enough to account for the fact that every recession comes with a unique magnitude.

Regarding the extraction of the factor from a set of observed information, each real activity indicator is assumed to be contemporaneously influenced by a common component and an idiosyncratic component. However, the treatment that each indicator receives depends on its corresponding frequency. In particular, indicators at the monthly frequency, $y_{i,t}^m$, can be expressed as:

$$y_{i,t}^m = \gamma_i f_t + u_{i,t}, \tag{4}$$

where γ_i denotes the associated factor loading and $u_{i,t}$ represents the idiosyncratic component. Instead, when dealing with indicators at the quarterly frequency, $y_{j,t}^q$, we follow Mariano and Murasawa (2003) and express quarter-on-quarter growth rates into month-on-month unobserved growth rates:

$$y_{j,t}^q = \frac{1}{3}y_{j,t} + \frac{2}{3}y_{j,t-1} + y_{j,t-2} + \frac{2}{3}y_{j,t-3} + \frac{1}{3}y_{j,t-4}. \tag{5}$$

Then, a quarterly growth rate can be expressed in terms of its idiosyncratic component and the common factor, as follows:

$$y_{j,t}^q = \gamma_j \left(\frac{1}{3}f_t + \frac{2}{3}f_{t-1} + f_{t-2} + \frac{2}{3}f_{t-3} + \frac{1}{3}f_{t-4}\right) + \\ + \frac{1}{3}u_{j,t} + \frac{2}{3}u_{j,t-1} + u_{j,t-2} + \frac{2}{3}u_{j,t-3} + \frac{1}{3}u_{j,t-4}. \tag{6}$$

Lastly, the idiosyncratic components, $u_{i,t}$, contain information that is exclusively associated to a particular indicator, after accounting for its degree of commonality with the rest of variables. They are assumed to follow autoregressive dynamics of order p,

$$u_{i,t} = \psi_{i,1}u_{i,t-1} + ... + \psi_{i,P}u_{i,t-P} + e_{i,t}, \quad e_{i,t} \sim \mathcal{N}(0, \sigma_i^2) \text{ i.i.d.} \tag{7}$$

Given the nonlinearities embedded in the model (1)-(7), we rely on Bayesian methods to produce inferences on both its parameters and latent variables. Let y_t denote the vector of observed monthly and quarterly indicators, and let $Y = \{y_t\}_{t=1}^T$ contain all the available data up to time T. Similarly, we define $Z = \{z_t\}_t^T$, where z_t denotes a vector containing latent states corresponding to the common factor f_t and idiosyncratic components $u_{i,t}$. Also, let $S = \{s_t\}_{t=1}^T$ be the collection of the latent regimes, and let $X = \{x_t\}_{t=1}^T$ contain the information on the unobserved adjustments to the mean growth rate during the abnormal episodes. All the

parameters that specify the model are collected in:

$$\theta = \left\{p, q, \mu_0, \mu_1, \sigma_f^2, \sigma_v^2, \{\gamma_i\}, \{\psi_{i,m}\}, \{\sigma_i^2\}\right\}.$$

The model is estimated using a modification of the Carter and Kohn (1994) algorithm, which simulates, in turn, the unobserved states Z, the unobserved mean adjustments X, and the indicators for abnormal episodes S. For a single run, given data Y and initial guesses θ^0, X^0, and S^0, the following iterative procedure is used:

1. Given Y, S_{i-1}, X_{i-1} and θ_{i-1}, generate Z_i from $P(Z|Y, S, X, \theta)$. This step follows Appendix 1 of Carter and Kohn (1994) and uses the definition of the common factor (1) and the observation equations (4) and (6).

2. Given Z_i, S_{i-1}, and θ_{i-1}, generate X_i from $P(X|Z, S, \theta)$. This step follows the same procedure as in Step 1, but now equation for the common factor (1) is treated as the observation equation, and equation (3) is treated as the law of motion for the unobserved state x_t.

3. Given Z_i, X_i, and θ_{i-1}, generate S_i from $P(S|Z, X, \theta)$. This step is based on equation (1) for the common factor and follows Appendix 2 of Carter and Kohn (1994).

4. Given Y, Z_i, X_i, and S_i, simulate θ_i using the standard prior distributions.

A more detailed description of the model and of the simulation procedure is provided in the Online Appendix.

3 Assessing Weakness Across Countries

In this section, we evaluate the performance of the proposed econometric framework to infer low economic activity regimes, or 'abnormal' episodes, both from real-time and international perspectives. First, we illustrate the advantages of allowing for recession-specific means in non-linear factor models (referred to as *time-varying mean*) by comparing their ability to anticipate turning points in real-time with the one associated to a regular nonlinear factor model, which assumes the same mean across all recessionary episodes (referred to as *constant mean*). Next, we show that our framework is flexible enough to be used for either advanced or emerging

economies. The literature involving the use of this type of frameworks to infer turning points in emerging economies is scarce. One possible reason for this is that modelling business cycles nonlinearities associated to emerging markets tends to be more challenging than for the case of developed countries due to a variety of features, such as strongly counter-cyclical current accounts or dramatic 'sudden stops' in capital inflows, Aguiar and Gopinath (2007), the role of country risk in the determination of emerging countries interest rates, Neumeyer and Perri (2005), or the role of patterns of production and international trade, Kohn et al. (2018).

3.1 Data

The proposed factor model, in equations (1)-(7), is independently fitted to twelve of the largest world economic regions, which together account for more than seventy percent of the world GDP. This set of regions include U.S., Euro Area, Japan, U.K., Canada and Australia, among advanced economies and, China, India, Russia, Brazil, Mexico and South Africa, among emerging markets. The list of the variables employed for each region is reported in Table 1. In general, we follow the original approach of Stock and Watson (1991), Chauvet and Piger (2008) or Camacho et al. (2018), mimicking national accounts procedures. We use supply side variables (usually, industrial production), internal demand variables (imports or sales), external demand (exports) and one additional variable, intrinsic of each economy. To all these monthly variables we add GDP. Those papers show that these small set of variables are reliable to address current conditions of the economy and comprise most relevant information to infer recessions in real time.

In addition, the main advantage of relying on real variables is that we capture all type of recessions, no matter if they have financial origin, energy prices, or any other cause. Whatever is the origin, if there is an effect on the economy, it has to be reflected in national accounts type of variables. However, it is worth emphasizing that the main purpose of this analysis is to illustrate the advantages of the proposed empirical framework with respect to alternative approaches. Therefore, improvements regarding the most adequate selection of variables for each of the different regions under consideration are left for further research. In all cases, the variables are seasonally adjusted, expressed in growth rates with respect to the previous period, and standardized prior to enter the corresponding model.

3.2 The Case of the United States

Dynamic factor models have been widely applied to the U.S. economy since it has been shown that they provide both accurate forecasts of GDP growth and inferences on the state of the economy in a real-time environment. On the one hand, Giannone et al. (2008) and Banbura et al. (2012), among others, have relied on linear factor models, that allow for mixed frequency data, to provide short-term forecasts of real GDP. On the other hand, Chauvet (1998) employs single-frequency nonlinear factor models, where the factor is subject to regime changes, with aim of providing timely inferences on turning points. Moreover, Chauvet and Piger (2008) show that Markov-switching dynamic factor models outperform alternative nonparametric methods when inferring U.S. recessions as dated by the NBER.

We estimate, in a Bayesian fashion, a constant mean factor model by extending the approach in Chauvet and Piger (2008) to allow for mixed frequency data, and include quarterly real GDP growth to the set of monthly real activity indicators. This extension constitutes our *constant mean* factor model. Our data starts in 1947 and ends in 2020, as shown in Table 1. This sample period allows us to evaluate the performance of the model over the last eleven NBER recessionary episodes.[5] The estimated probability of low real activity regime, $Pr(s_t = 1)$, is shown in Chart A of Figure 1, along with the data on GDP growth, for comparison purposes. Although the estimated probability reaches values close to one during eight of the eleven recessionary episodes, the model does not provide a high recession probability for the three remaining recessions; 1969:12–1970:11, 1990:07–1991:03, and 2001:03–2001:11. This is because these three recessions seem to be either less severe, less persistent, or both, than the rest. Therefore, since the model assumes that the mean growth across all recessionary episodes is the same based on the entire sample, the estimated mean of the factor during recessions is dominated by the eleven stronger and more persistent recessions, and consequently, the model fails to produce a high probability attained to the three remaining recessionary episodes.

In order to account for the fact that some U.S. recessions could be substantially more severe than others, we estimate the *time-varying mean* factor model proposed in this paper, and plot its associated probability of low growth regime in Chart B of Figure 1. The figure shows that the estimated probability reaches values close to one during all the NBER recessions, with no

[5] In particular, the last eleven U.S. recession, as defined by the NBER, are dated as follows: 1948:11–1949:10, 1953:07–1954:05, 1957:08–1958:04, 1960:04–1961:02, 1969:12–1970:11, 1973:11–1975:03, 1980:01–1980:07, 1981:07–1982:11, 1990:07–1991:03, 2001:03–2001:11, 2007:12–2009:06.

exceptions, outperforming the *constant mean* factor model. The reason for the success of the proposed framework relies on the premise that the growth rate during each recession is unique, in line with Eo and Kim (2016). However, unlike these authors, our approach is more parsimonious and simply assumes that recession means have two components. The first component is deterministic and given by the estimated parameter μ_1, which provides an assessment about the average growth across all recessionary episodes in the sample. Instead, the second component is random, given by the normally distributed variable x_t, which provides the uniqueness associated to each recessionary episodes. The random term x_t can be interpreted as deviations from the deterministic component μ_1. Hence, negative (positive) values of x_t indicate weaker (stronger) growth than the average across all recessionary episodes, μ_1. Chart A of Figure 21, in the Appendix, plots the empirical mean and median of the random variable x_t over time for the case of U.S., illustrating the need for an adjustment factor, especially, during the 1973:11–1975:03 and 2007:12–2009:06 recessions.

Next, we turn to evaluate the performance of the two competing factor models in a real-time environment. First, we estimate both models with revised data from 1947:02–1989:12. Second, we perform recursive estimations with unrevised (that is, real-time) vintages of data, from 1990:01 until 2019:08, adding one month of information at every time. The real-time vintages associated the variables in the model were retrieved from the Archival of the FRED economic datase.[6] The estimated real-time probabilities of low activity regime associated to both models are plotted in Figure 2. Several features deserve to be commented. First, the real-time inferences, obtained with the *constant mean* factor model, are able to provide a better track of the last three NBER recessions than the full-sample (1946–2019) inferences obtained with the same model. This is because inferences on a recession in the present are not 'contaminated' by any information (for example, deepness) associated to recessions in the future. Second, the real-time probabilities coming from the *constant mean* factor model accurately infer the end of the recessions. However, they fail to provide a 'timely alarm' for the beginning of the recessionary episodes. This feature is aligned with the results in Camacho et al. (2018), who rely on a classical estimation approach. Third, the real-time probabilities obtained with the *time-varying mean* factor model tend to quickly rise to values close to one at the beginning of the recessions, and drop to values close to zero at their end. This result emphasizes the usefulness of the proposed approach in providing timely updates of the state of the economy in the real-time environment

[6] https://alfred.stlouisfed.org/.

that policy makers and investors face.

3.3 The Case of the Euro Area[7]

Dynamic factor models have been also applied for nowcasting purposes in the euro area, either from a single economy perspective (Banbura et al. (2011)) or for individual member countries (Runstler et al. (2009)). More related to our study, Camacho et al. (2014) provide a nonlinear extension, which allows the mean factor to switch between regimes of high and low growth, with the aim of inferring the state of the euro area economy in real-time.

Producing accurate inferences on the state of the euro area economy is associated to an important challenge regarding the differences in the definition of a low activity regime. According to the Euro Area Business Cycle Dating Committee of the Centre for Economic Policy Research (CEPR), since the introduction of the euro, there have been two episodes that can be technically categorized as recessions; 2009:03–2010:10 and 2012:11–2015:10. While during the first period the average growth was -0.9%, in the second one the average growth reached only to -0.2%. In other words, the 2009:03–2010:10 recession was about 4.5 times more severe than the 2012:11–2015:10 recession. As we illustrate below, this particular feature has important implications for the performance of nonlinear factor models in defining regimes of low and high growth.

We estimate a *constant mean* factor model for the Euro Area, with the corresponding data reported in Table 1. For the sake of space, the estimated probability of low growth regime is plotted in Chart A of Figure 10 in the Online Appendix. The model attains a high probability of low growth only to the slowdown associated to the Great Recession, and fails to detect other periods of negative (2012–2013) or weak (2001–2004) output growth. This is because during the Great Recession, the Euro Area exhibited an unprecedented deterioration in real activity, which fully dominates the estimated low mean growth. Hence, similarly to the case of the U.S., the assumption that all recession are alike turns to be detrimental to accurately infer regimes of low real activity. Next, we evaluate the performance of the proposed *time-varying mean* factor model, and plot the probability of low growth in Chart B of Figure 10. The estimates show that when allowing for heterogeneous means, the model is able to attain a high probability of low growth to all the episodes associated to either negative or weak output growth in the sample.[8].

[7]The Euro Area model has been estimated in the context of the task force of the Eurosystem on nonlinear tools.

[8]In Chart B of Figure 21 of the Online Appendix, it can be seen that the adjustment of the mean growth during the period associated to the Great Recession was sizeable in comparison to the other times of weak activity, due

3.4 Other Advanced Economies

As just pointed, factor models subject to regime changes have been successfully used for the U.S. and Euro Area economies. Here, we evaluate how this type of models perform when facing data of a different nature associated to other advanced economies.

Australia

The growth of real GDP in Australia has generally remained at positive values since the mid 1990s, with only a few exceptional quarters of negative growth. This feature entails a significant challenge in assessing the state of its economy based on regime-switching models previously used in the literature. To illustrate this point, we estimate the *constant mean* factor model with the Australian data reported in Table 1. The associated probability of low real activity is plotted in Chart A of Figure 11, reporting values between 0.2 and 0.7, and therefore, showing that this model is not able to clearly identify the presence of more than one regime associated to the underlying data. Next, we estimate the *time-varying mean* factor model, and plot the associated probability of low real activity in Chart B of Figure 11. The estimated inferences show the *time-varying mean* model provides a clearer identification of a low activity regime, occurred in 2009, than the *constant mean* model.

Canada

Inferring the state of the Canadian economy is expected to face similar challenges to the case of the U.S., given their close ties.[9] We estimate the *constant mean* factor model with the Canadian data reported in Table 1. The estimated probability of low real activity is plotted in Chart A of Figure 12. Notice how the downturn in real activity associated to the Great Recession dominates the regime inferences, since the model only provides high probability to that specific period. However, as the figure shows, GDP growth has exhibited several additional episodes of weakness, which are totally missed due to the assumption that all recessions are alike. Next, we estimate the *time-varying* factor model with Canadian data, and plot the associated probability of low real activity in Chart B of Figure 12. The changes with respect to the Chart A are apparent. The *time-varying* factor model is able to produce monthly probabilities that match

to its severity

[9] In the previous work by Chernis and Sekkel (2017), dynamic factor models are employed to produce nowcasts of the Canadian GDP growth. Although, to the best of our knowledge, ours is the first study that uses nonlinear factor models to infer its regimes of high and low real activity.

fairly well with episodes of either weak or negative GDP growth, constituting a more reliable tool for assessing the state of the economy than the *constant mean* factor model.

Japan

Next, we focus on the economy of Japan, whose real GDP was significantly contracted during the Great Recession in comparison with other temporary downturns occurred since the mid 1990s. We estimate the *constant mean* factor model with Japanese data, and plot the associated probability of low activity in Chart A of Figure 13. The estimated inferences identify two periods of low real activity, corresponding to the downturns of 2009 and 2012. Instead, when relying on the *time-varying mean* factor model, additional episodes of low real activity are identified, as shown in Chart B of Figure 13. Notice that these additional episodes are associated to smaller, but still negative, declines in output growth than the ones occurred in 2009 and 2012. This illustrates the ability of our framework to identify economic downturns associated to heterogeneous deepness.

United Kingdom

Since the 'Brexit' referendum of 2016, the U.K. economy has been subject to a high level of uncertainty, which has increased the interest in inferring a potential upcoming recession. However, recent GDP downturns, occurred since the mid 1980s, have been in general substantially smaller than the contraction exhibited during the Great Recession. This feature could preclude a model to accurately infer the next recession if it is of a smaller magnitude than the one observed in 2008-2009. We estimate the *constant mean* factor model for U.K. data, and plot the corresponding probability of low activity in Chart A of Figure 14. As expected, this model is only able to infer the significant downturn associated to the 2008-2009 recession, missing other periods of negative GDP growth. Next, we estimate the *time-varying mean* factor model, and plot the associated probability of low activity in Chart B of Figure 14. The estimates attain a relatively high probability to additional periods associated to either low or negative output growth.

3.5 Emerging Markets

There is a flourishing literature focused on employing dynamic factor models to provide nowcasts of activity in emerging markets. This framework has been applied for Brazil (Bragoli et al. (2015)), Mexico (Corona et al. (2017)), Russia (Porshakov et al. (2016)), India (Bragoli and Fosten (2017)), and China (Yiu and Chow (2010)). Also, some works focus comparing the performance of factor models in more than one country. This is the case of Cepni et al. (2019a) and Cepni et al. (2019b) who compare address the cases of Brazil, Indonesia, Mexico, South Africa, and Turkey. Also, Dahlhaus et al. (2015) encompass a wider sample of countries, by also including Russia and China into the analysis. The overall message of these works, is that factor models also tend to be successful in providing accurate short-term forecast of output growth for this type of countries. However, the literature on assessing the state of the emerging economies is rather scarce. In this section, we employ the proposed framework to provide timely inferences on low real activity regimes for six of the largest emerging markets; Brazil, Mexico, Russia, India, China and South Africa.

For the case of Brazil, Chauvet (2001) proposes the use of a single-frequency factor model subject to regime-changes with the aim of inferring recessions, with data prior to 2000, finding several episodes of low real activity. We fit the *constant mean* factor model to Brazilian data reported in Table 1, with data starting in 1996 until the present time. The estimated probabilities of low activity are plotted in Chart A of Figure 15, showing that the inferences are dominated by the acute downturn associated to the Great Recession, reaching a quarterly growth of around -4 percent. Consequently, the model is not able to categorize as low activity regimes to several episodes of negative, or even close to zero, output growth. Instead, the probabilities obtained with the *time-varying mean* factor model provides a more accurate assessment of weak activity periods of the Brazilian economy, such as the one between 2014 and 2015. Also, the correction in the recession mean growth needed to improve the inference exhibits different magnitudes and directions, as can be seen in Chart D of Figure 21, indicating a strong idiosyncracy of real activity downturns in Brazil.

We also apply the proposed framework to the cases of Mexico, Russia, India, China and South Africa and plot the corresponding probabilities of low activity regime in figures, 16, 17, 18, 19, and 20, respectively. In all five cases, the results indicate that the *time-varying mean* factor model outperforms the *constant mean* model in that the former is able to make a better

track of weak real activity periods in emerging markets, which are aligned with the downturns in GDP growth. All these results emphasize the flexibility of our approach in adapting to economies with substantially diverse types of activity dynamics to provide a robust tracking of its strength.

4 Assessing Global Weakness

The Great Recession carried out severe and long-lasting negative consequences for world economy. Recently, the IMF has called the attention for synchronized global slowdown in economic activity since many of the largest economies are exhibiting decelerations in their output growth pace (IMF, 2019) and different institutions consider that the coronavirus crisis has put the economy at the verge of a recession. Therefore, inferring the state of the world economy on a timely basis is of great importance. In a recent study, Ferrara and Marsilli (2018) propose a framework to produce short-term forecasts of the global economic growth by also using factor models, which are fitted to economic indicators from different advanced and emerging economies. Although, the authors rely on a linear approach, since they only focus on nowcasting, and not on inferring the state of the global economy.

The framework proposed in this paper has been shown to provide accurate and timely assessment about the weakness of the economic activity in some of the largest advanced and emerging economies. In this section, we propose a simple way to combine all those assessments into a single index that proxies the weakness of the world economy and that can be updatable in real-time. The purpose of the proposed index is threefold; (i) measuring the weakness of the world economy, (ii) identifying the main underlying sources of global weakness, and (iii) providing risk assessments of global downturns associated to different intensities.

4.1 Dynamics and Sources of Weakness

To provide a comprehensive view of the evolving heterogeneity of the economic weakness across different regions, the information on their corresponding probabilities of low activity are plotted in world maps for selected periods. Chart A of Figure 3 shows the global situation for 2008:11, around the middle of the last global recession. As expected, all the regions under consideration reported a probability of low activity close to one, exhibiting a high synchronization in a 'bad' state. Instead, Chart B plots the global situation for 2010:01, the beginning of the year with the strongest annual world GDP growth since the Great Recession (5.4 percent). This

is also a very homogeneous period, however, in this case all the regions reported a probability of low activity close to zero, exhibiting a high synchronization in a 'good' state. However, not all time periods are accompanied by such a high degree of synchronicity. In general, there is substantial heterogeneity regarding the state of the economy across regions. An example of that is shown in Chart C, which plots the situation for the last period in our sample, 2020:02. Notice that some regions, such as the Euro Area, currently show a position substantially weaker than others that face a stronger activity. However, the most striking feature of this map is the high weakness of the Chinese economy, induced by the coronavirus crisis. An advantage of this map is that it can be updated every day that a new datum, associated to any of the regions under consideration, is published. These updates would help to reassess the weakness of a given economy in global comparative terms. The entire sequence of maps for the period 2003:04-2020:02 is available online.[10]

We are interested in providing a single statistic that summarizes the state of the global economy, and that additionally can be (i) updated in real-time, (ii) decomposed into its regional contributions, (iii) useful to quantify risks, and (iv) simple to interpret. Therefore, we proposed the Global Weakness Index (GWI) which consists on a weighted average between the probabilities of low activity associated to each of the K regions under consideration. Since the models are estimated in a Bayesian fashion, we are able to reproduce many replications associated to the realization of a low activity regime for each region, that is, $s_{\kappa,t}^{(l)}$, and for $\kappa = 1, ..., K$, and $l = 1, ..., L$, where K is the number of countries and L is the number of draws. L should be large enough to ensure convergence in the associated posterior density. Hence, the l-th replication of the GWI is given by,

$$GWI_t^{(l)} = \sum_{\kappa=1}^{K} \omega_{\kappa,t} s_{\kappa,t}^{(l)}, \tag{8}$$

where $\omega_{\kappa,t}$ denotes the time-varying weights associated to each region based on its evolving economic size relative to the world GDP. The collection of all the replications $\{GWI_t^{(l)}\}_{l=1}^{l=L}$ constitutes the simulated density of the index at time t, from which point estimates along with any percentile, to measure its uncertainty, can be easily computed. Notice that, by construction, the GWI is bounded between zero and one. That is, the index would take the upper (lower) bound value of one (zero) when the probabilities of weak activity associated to all the regions under consideration are equal to one (zero), implying the highest (lowest) degree of global

[10] It can be found at https://sites.google.com/site/daniloleivaleon/global_weakness.

weakness.

In Chart A of Figure 4, we plot the Global Weakness Index, along with the world GDP growth, for comparison purposes.[11] There are several important features. First, notice that the GWI starts to rapidly increase during 2008, reaching a value of 0.8 in October of the same year, indicating clear signs of a global contraction. Second, as the GWI increases during 2008, the corresponding credible set shrinks, indicating a high synchronization in a 'bad' state.[12] Third, the GWI anticipates the exit of the last global recession by dropping to values close to zero around July 2009. Fourth, the index also detects two episodes of moderate weakness for the world economy. The first one took place between the late 2015 and the early 2016, period of slower growth in emerging markets and gradual pickup in advanced economies, as characterized by the IMF. The second episode of moderate weakness is the present one. There is a moderate increase in weakness since 2018 that skyrockets with the information about coronavirus crisis, taking the index to its largest value since the beginning of the Great Recession, in the early 2008.

The full-sample estimates of the GWI, shown in Chart A of Figure 4, are of high importance in order to compare the current state of the world economy with respect to the past, based on all available information. However, it is also relevant addressing whether the GWI index is able to provide accurate real-time assessments of the state of the world economy, that is, by using only the available information at the moment of the estimation. In doing so, we recursively estimate all the models associated to the 12 economic regions under consideration by including one month of information at a time. Our estimations of the models are based on expanding windows, staring at the beginning of the sample for each region, as reported in Table 1, and ending in periods from 2007:01 until 2020:02.[13] Next, we compute the GWI associated the each of the recursive estimations, and collect the last available estimates for each vintage of data. The sequence of these collected GWI estimates, shown in Chart B of Figure 4, represent the assessments that our proposed framework provides about the state of the world economy at every period, constructed by using only the available information at that point in time. Notice that the real-time GWI index resembles fairly well the full-sample estimates, indicating a robust performance in inferring regimes of low activity in a timely fashion. This feature can

[11] The world GDP is taken from the IMF database.

[12] The credible set of the GWI is define by the percentiles 16th and 84th of the simulated distribution.

[13] Due to the complexity of the international environment we are dealing with, there are data availability constraints, and therefore, our estimations do not take into account data revisions of the associated variables.

be particularly observed at the beginning of the Great Recession, where the GWI provided a strong real-time alert, taking values higher than 0.5 during the first months of 2008.

Notice that every day that a new figure of data on the variables associated to the different regions (in Table 1) is released the GWI can be updated. To the best of our knowledge there is no other model-based index that provides updates on the state of the global economy with such a high frequency. Yet, there is a non-model-based index that is able to proxy the overall 'sentiment' of agents about the likelihood of an upcoming global recession. This index can be computed by counting the number of web searches of the words "Global Recession" performed by internet user from all over the world, and therefore, can also be updated at the daily frequency. Figure 5 plots the web search index, which is associated to agents' inference about a global recession, along with the GWI, which is based on information of real economic activity. The figure shows that despite both indexes pick up around the last global recession, as dated by Kose et al. (2020), the GWI substantially leads the web search index. In particular, the web search index increases once the last global recession was almost in the middle of its duration, and substantially declined (below levels of 0.2) about a year after the beginning of the last global expansion. Also, while the web search index has remained relatively unchanged since 2010, the GWI has indicated signs of moderate economic global weakness at different points in time. These results provide comparative evidence in favor of the timeliness of the GWI to infer global downturns.

The contributions of advanced and emerging economies to the total world GDP have exhibited sizable changes over the last years. While, for example, the shares of U.S. and Euro Area have declined, the relative economic importance of China and India has surged with time. This evolving composition plays a important role when disentangling the main sources of weakness in global activity. As defined in Equation (8), the GWI can be easily decomposed into the contributions associated to each economic region. Each of these contributions has two components. First, the likelihood of falling in a low activity regime, $E[s_{\kappa,t}]$, and second, the economic importance of such likelihood for the world GDP, $\omega_{\kappa,t}$. The product of these two components helps to identify the main contributors of the degree of weakness of the global economy, either it is high or low.

In Figure 6, we plot the GWI along with its corresponding regional contributions, which are normalized to sum up to one for every time period for ease of interpretation. The figure shows the substantial importance of the U.S. in the deterioration of global economic conditions at the

beginning of the last global recession, around the end of 2007. However, in 2008 the relative contribution all the other regions, in particular, advanced economies, starts to rise, yielding a more uniform composition during the middle that global recession, by 2009. This pattern is consistent with a sequential propagation of recessionary shocks. The subsequent recovery, which started around late 2009, and posterior expansion, since 2010, was instead characterized by a degree of global weakness close to zero, where the main contributors were emerging markets.

This buoyant global economic stance lasted for about a year. Since 2011 the GWI experienced slight, but sustained, increases, driven by the Japanese economy due to a sequence of unexpected events, such as, an earthquake, a tsunami, and the Fukushima's nuclear crisis. In 2012 the GWI increased another point, reaching to 0.3, although with a different composition. This time, the main contributor was the Euro Area due to the sovereign debt crisis. During 2015, there was another slight increase in the GWI, which can be mainly attributed to Russia due to the international economic sanctions and oil shocks that were highly detrimental for its financial conditions. Lastly, the decomposition also illustrates the large impact that the recent deterioration in Chinese economic conditions have had on the increasing weakness of the global economy. Overall, the GWI is shown to provide a narrative of events that have led to either slight or substantial increases in the weakness of the global economy.

4.2 Monitoring Global Risks

In a recent work, Adrian et al. (2019) illustrate the importance of evaluating downside risks of U.S. output growth associated to tighter financial conditions. The authors rely on quantile regressions to model the conditional predictive densities of real activity. Thereafter, this methodology has also been applied to a wide variety of individual countries for macroeconomic surveillance purposes (Prasad et al. (2019)). Assessing the likelihood of upcoming extreme events, or "macroeconomic disasters", given the current conditions, is crucial for policymakers. Although, this task becomes more challenging when the target to be monitored is the world economy, as a whole. This is due to the lack of, relatively, high frequency economic data at the world level.

In this section, we employ the proposed GWI as a tool for monitoring risks at the global level and in real-time. Also, due to the way in which the GWI is constructed, it is straightforward to provide timely assessments about two important features of the world economy. First, the evaluation of risks associated to a state of low global activity. Second, the regional contributions

associated to such risks. Figure 7 shows the weakness stance of the global economy during four selected periods. First, Chart A shows the situation at the beginning of the last global recession (2008M03), where most of the mass of the GWI distribution started to displace towards the right, suggesting an upcoming weakening of the global economy. Also, corresponding the radar chart indicates that most of such a weakening was originated in the U.S. economy. Chart B shows the same type of information, but for a period around the middle of the last global recession (2009M01), where most of the mass of the GWI distribution was compressed at values close to one, indicating a severe global downturn. The associated radar chart reveals that the GWI composition in this period was relatively homogeneous between the largest world economies, that is, U.S., the Euro Area and China, due to the international propagation of contractionary shocks. Chart C shows the global risk assessment during a period of buoyant recovery (2009M12), which is reflected in GWI distribution, concentrated in values close to zero. Interestingly, not only the U.S. and the Euro Area were the drivers of this trend, but also the economies of Japan and Russia significantly contributed. Lastly, Chart D plots the current situation (2020M02), which suggests increasing risks of high level of global weakness, with China being the main driver due to the coronavirus outbreak.

The information contained in the time-varying GWI distributions, plotted in Figure 7, can be also useful to quantify the probability associated to specific scenarios of weakness in global activity. For example, if one is interested in assessing the probability that the weakness of the global economy would exceed a low level. In this case, we define a low level by a value of $GWI_t = 0.3$, and compute the associated cumulative density. Similarly, we compute the probability the weakness of the global economy would exceed a medium, high, and very high level, defined by values of 0.5, 0.7, and 0.9, of the GWI, respectively. These values are used just as reference and can be changed based on the judgement of the policy markers or pundits.

Chart A of Figure 8 plots the time-varying probabilities associated to the scenarios in which the global weakness is higher than the selected thresholds. As expected, the larger is the GWI threshold, the less likely tends to be such an scenario. The probability of exceeding a low global weakness level varies substantially over time and, with the exception of the periods around 2010 and 2017, it tends to be a highly likely scenario. Instead, the probability of exceeding a high level of global weakness tends to be relatively low over time, with the exceptions of the period between 2008 and 2009. Lastly, the probability of a 'catastrophe', that is, when the global weakness exceeds a very high level reaches to values close to one at the beginning of 2009, and

have remained close to zero during the rest of the sample.

To provide a broader perspective of these probabilistic assessments, in Chart B of Figure 8, we plot the same information, but allowing for a continuum of the GWI thresholds, information that can be interpreted as the density function of the global economic weakness in every period of time. The plotted surface illustrates the constantly changing nature of global economic risks. It is worth emphasizing that all these probabilistic assessments are constructed only with the available (revised) data at the time of the estimation. To illustrate the readiness of the GWI, we zoom into the period before and during the Great Recession. That is, we slice the surface of global weakness at selected time periods between 2007 and 2009 and plot this information in Figure 9, showing that as the world economy enters the last global recession, the curves relating degree of weakness with probability of occurrence change from concave, in February 2007, to convex, in January 2009. Therefore, this displacements of the curves indicate a progressive rise in global economic risks. These results illustrate that GWI is able to provide a robust and timely evaluation of economic risks associated to the world economy.

5 Conclusions

Motivated by recent events that signal a potentially global synchronized slowdown, we propose an econometric framework able to provide timely and accurate real-time inferences about the state of the world economy. We introduce a mixed frequency dynamic factor model that allows for heterogeneous deepness across recessionary episodes. The proposed model is fitted to twelve of the world's largest economic regions. Our estimates show that allowing for heterogeneous recessions turns to be crucial in accurately inferring periods of weak real activity growth associated with both advanced and emerging economies, outperforming frameworks previously proposed in the literature. Next, the estimated regional inferences are summarized into a Global Weakness Index (GWI), which is able to provide daily real-time updates of the global economy strength, its underlying sources, and risk assessments, as new information across the regions is released.

The proposed framework for monitoring the state of the world economy can be extended in different ways. For example, by determining the most adequate set of economic indicators associated to each region in order to maximize the accuracy when inferring region-specific recessions. Also, a wider range of regions can be incorporated in the construction of the global

weakness index with the aim of sharpen the accuracy when inferring world recessions.

References

Adrian, T., N. Boyarchenko, and D. Giannone (2019). Vulnerable growth. *American Economic Review 109*(4), 1263–1289. 4.2

Aguiar, M. and G. Gopinath (2007). Emerging market business cycles: The cycle is the trend. *Journal of Political Economy 115*(1), 69–102. 1, 3

Banbura, M., D. Giannone, and L. Reichlin (2011). Now-casting and the real-time data flow. *Oxford Handbook on Economic Forecasting,*, 193–224. 3.3

Banbura, M., M. Modugno, and L. Reichlin (2012). Now-casting and the real-time data flow. *Handnook of Economic Forecasting 2*. 3.2

Barnett, W., M. Chauvet, and D. Leiva-Leon (2016). Real-time nowcasting of nominal gdp with structural breaks. *Journal of Econometrics 191*, 312–324. 1

Bragoli, D. and J. Fosten (2017). Nowcasting indian gdp. *Oxford Bulletin of Economics and Statistics 80*(2), 259–282. 3.5

Bragoli, D., L. Metelli, and M. Modugno (2015). The importance of updating: Evidence from a brazilian now-casting model. *OECD Journal: Journal of Business Cycle Measurement and Analysis 1*, 5–22. 3.5

Burns, A. and W. Mitchell (1946). *Measuring Business Cycles*. NBER Book Series Studies in Business Cycles. New York. 1

Camacho, M., G. Perez-Quiros, and P. Poncela (2018). Markov-switching dynamic factor models in real time. *International Journal of Forecasting 34*(4), 598–611. 3.1, 3.2

Camacho, M., G. P. Quiros, and P. Poncela (2014). Green shoots and double dips in the euro area: A real time measure. *International Journal of Forecasting 30*(3), 520–535. 1, 3.3

Carter, C. K. and R. Kohn (1994). On gibbs sampling for state space models. *Biometrika 81*(3), 541–553. 2, 1, 3, A.2

Cepni, O., E. Guney, and N. Swanson (2019a). Forecasting and nowcasting emerging market gdp growth rates: The role of latent global economic policy uncertainty and macroeconomic data surprise factors. *Journal of Forecasting*, Forthcoming. 3.5

Cepni, O., E. Guney, and N. Swanson (2019b). Nowcasting and forecasting gdp in emerging markets using global financial and macroeconomic diffusion indexes. *Journal of International Forecasting 33*(2), 555–572. 3.5

Chauvet, M. (1998). An econometric characterization of business cycle dynamics with factor structure and regime switches. *International Economic Review 39*(4), 969–996. 1, 3.2

Chauvet, M. (2001). A monthly indicator of brazilian gdp. *Brazilian Review of Econometrics 21*(1), 1–47. 3.5

Chauvet, M. and J. Piger (2008). A comparison of the real-time performance of business cycle dating methods. *Journal of Business & Economic Statistics 26*, 42–49. 2, 3.1, 3.2

Chernis, T. and R. Sekkel (2017). A dynamic factor model for nowcasting canadian gdp growth. *Empirical Economics 53*(1), 217–234. 9

Corona, F., G. González-Farías, and P. Orraca (2017). A dynamic factor model for the mexican economy: are common trends useful when predicting economic activity? *Latin American Economic Review 26*(7), 1–35. 3.5

Dahlhaus, T., J.-D. Guenette, and G. Vasishtha (2015). Nowcasting bric+m in real time. *International Journal of Forecasting 33*(4), 915–935. 3.5

Eo, Y. and C.-J. Kim (2016). Markov-switching models with evolving regime-specific parameters: Are postwar booms or recessions all alike? *Review of Economics and Statistics 98*(5), 940–949. 1, 2, 3.2

Ferrara, L. and C. Marsilli (2018). Nowcasting global economic growth: A factor-augmented mixed-frequency approach. *The World Economy 42*(3), 846–875. 4

Giannone, D., L. Reichlin, and D. Small (2008). Nowcasting: The realtime informational content of macroeconomic data. *Journal of Monetary Economics 55*(4), 665–676. 3.2

Hamilton, J. (2019). Measuring global economic activity. *Journal of Applied Econometrics* (Forthcoming). 4

Hamilton, J. D. (1989). A new approach to the economic analysis of nonstationary time series and the business cycle. *Econometrica: Journal of the Econometric Society*, 357–384. 1, 2

IMF (2019). *World Economic Outlook, October 2019: Global Manufacturing Downturn, Rising Trade Barriers*. IMF. 4

IMF (2020). *Press Release*. Number 20/61, February 22. International Monetary Fund. 1

Jerzmanowski, M. (2006). Empirics of hills, plateaus, mountains and plains: A markov-switching approach to growth. *Journal of Development Economics 81*(2), 357–385. 1

Kilian, L. (2019). Measuring global real economic activity: do recent critiques hold up to scrutiny? *Economics Letters 178*, 106–110. 4

Kohn, D., F. Leibovici, and H. Tretvoll (2018). Trade in commodities and business cycle volatility. *Federal Reserve Bank of St. Louis Working Paper* (2018-005B). 3

Kose, A., N. Sugawara, and M. Terrones (2020). Global recessions. *CEPR Working Papers 14397*. 4.1

Mariano, R. S. and Y. Murasawa (2003). A new coincident index of business cycles based on monthly and quarterly series. *Journal of Applied Econometrics 18*(4), 427–443. 2, A.1

Neumeyer, P. and F. Perri (2005). Business cycles in emerging economies: the role of interest rates. *Journal of Monetary Economics 52*(2), 345–380. 3

OECD (2020). *Newsroom: Global Economy faces gravest threat since the crisis as coronavirus spreads*. Number March 2. Organisation for Economic Co-operation and Development. 1

Porshakov, A., A. Ponomarenko, and A. Sinyakov (2016). Nowcasting and short-term forecasting of russian gdp with a dynamic factor model. *Journal of the New Economic Association 30*(2), 60–76. 3.5

Prasad, A., S. Elekdag, P. Jeasakul, R. Lafarguette, A. Alter, A. Feng., and C. Wang (2019). Growth at risk: Concept and application in imf country surveillance. *IMF Working Papers* (19-36). 4.2

Runstler, G., K. Barhoumi, S. Benk, R. Cristadoro, A. Den Reijer, A. Jakaitiene, P. Jelonek, A. Rua, K. Ruth, and C. Van Nieuwenhuyze (2009). Short-term forecasting of gdp using large datasets: a pseudo real-time forecast evaluation exercise. *Journal of Forecasting 28*(7), 595–611. 3.3

Stock, J. and M. Watson (1991). A probability model of the coincident economic indicators. *Leading Economic Indicators: New Approaches and Forecasting Records*. 3.1

Yiu, M. and K. Chow (2010). Nowcasting chinese gdp: information content of economic and financial data. *China Economic Journal 3*(3), 223–240. 3.5

Figure 1: United States

(a) Probability of low economic activity regime: Constant mean model

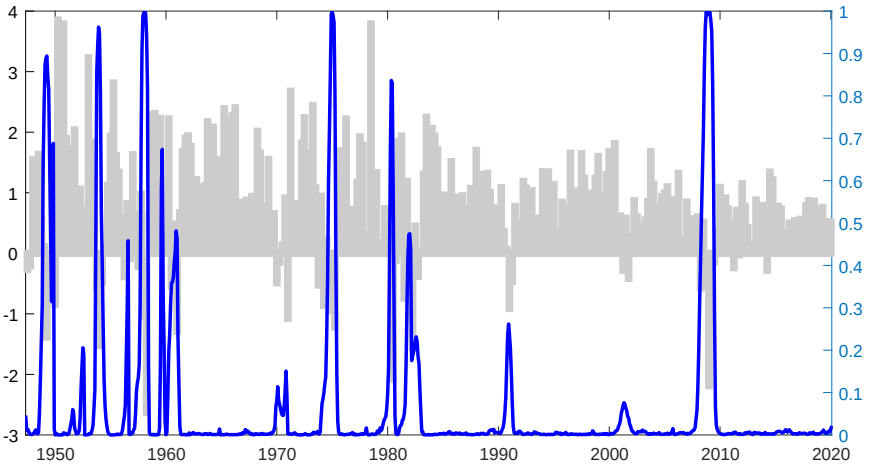

(b) Probability of low economic activity regime: Time-varying mean model

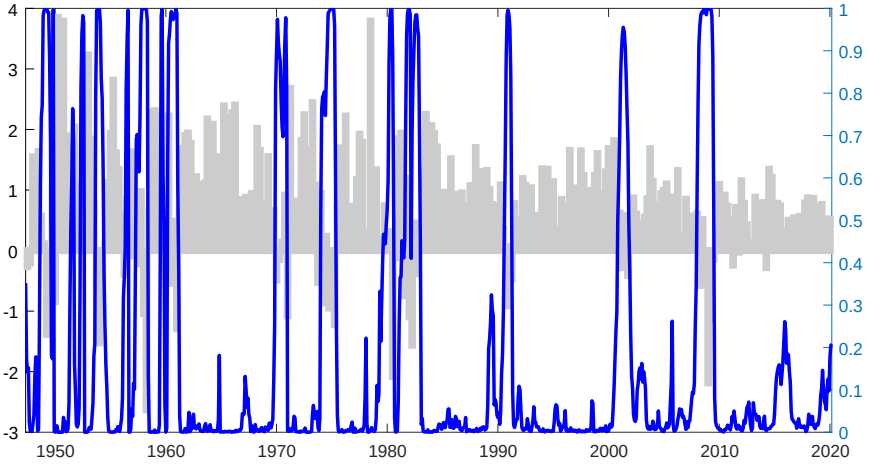

Note: The blue solid line (right axis) plots the monthly probability of low real activity regime, $Pr(s_t = 1)$, for the corresponding model, and the grey bars (left axis) represent the real GDP quarterly growth.

Figure 2: United States: Real-Time Performance

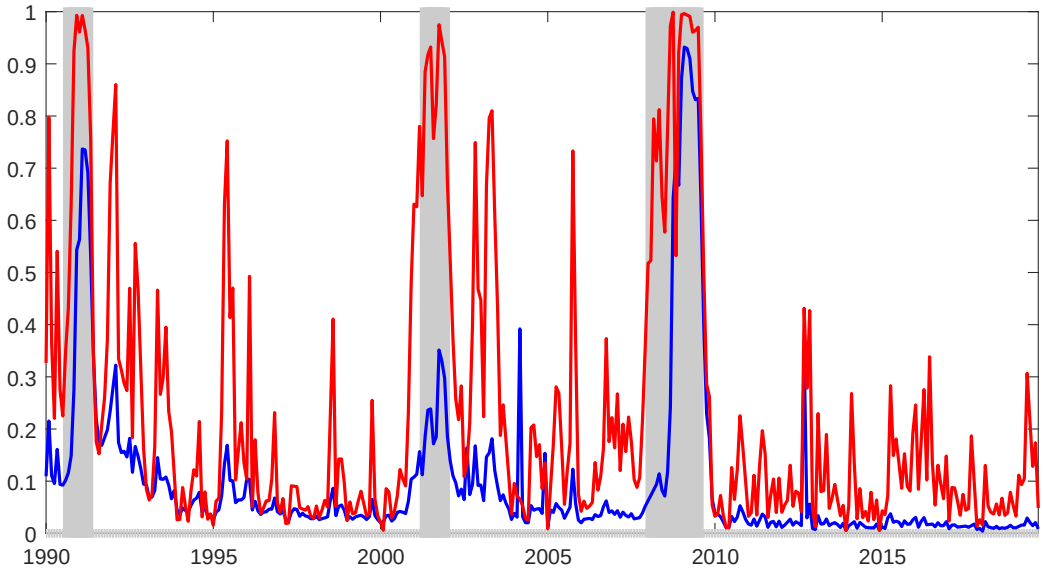

Note: The figure plots the probabilities of low real activity computed with recursive out-of-sample exercises and with real-time data, that is, by employing the exact amount and type of information available at the time of the estimation. The blue line plots the probability computed with the *constant mean* factor model, while the red line plots the probability computed with the *time-varying mean* model. The dashed area correspond to recession periods, as dated by the NBER.

Figure 3: Weakness Across Countries

(a) Middle of the Last Global Recession

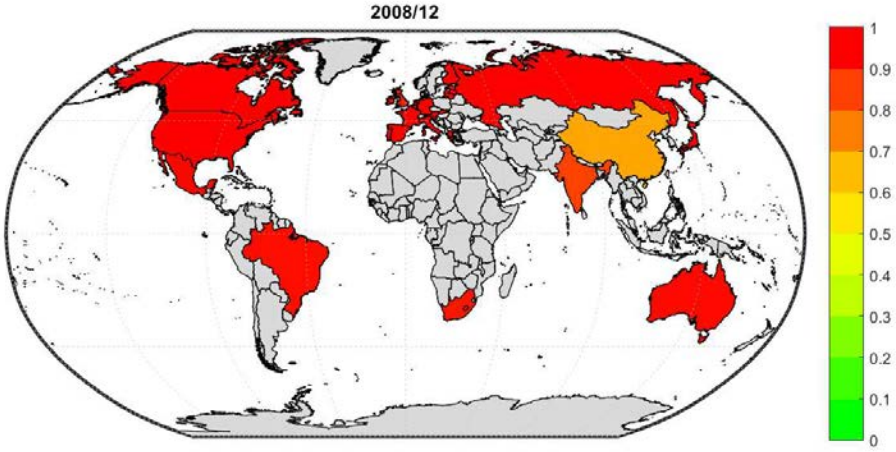

(b) Beginning of the Last Global Expansion

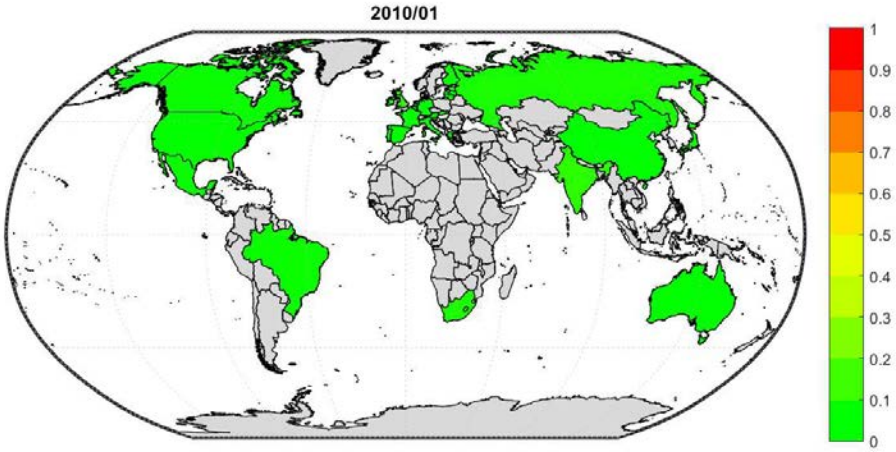

(c) End of Sample

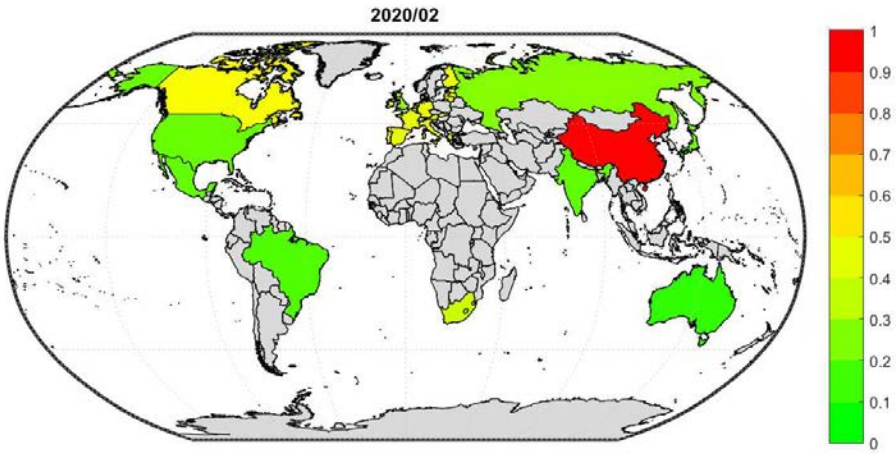

Note: The heatmap of the world plots the overall pattern of the probabilities of low economic activity regime $Pr(s_t = 1)$ for specific periods. The darker (lighter) the area, the higher (lower) the probability of low economic activity. The animated sequence of world heatmaps, from 2003:04 until 2020:02, can be found at: https://sites.google.com/site/daniloleivaleon/global_weakness.

Figure 4: Global Weakness Index

(a) Full-Sample Estimates

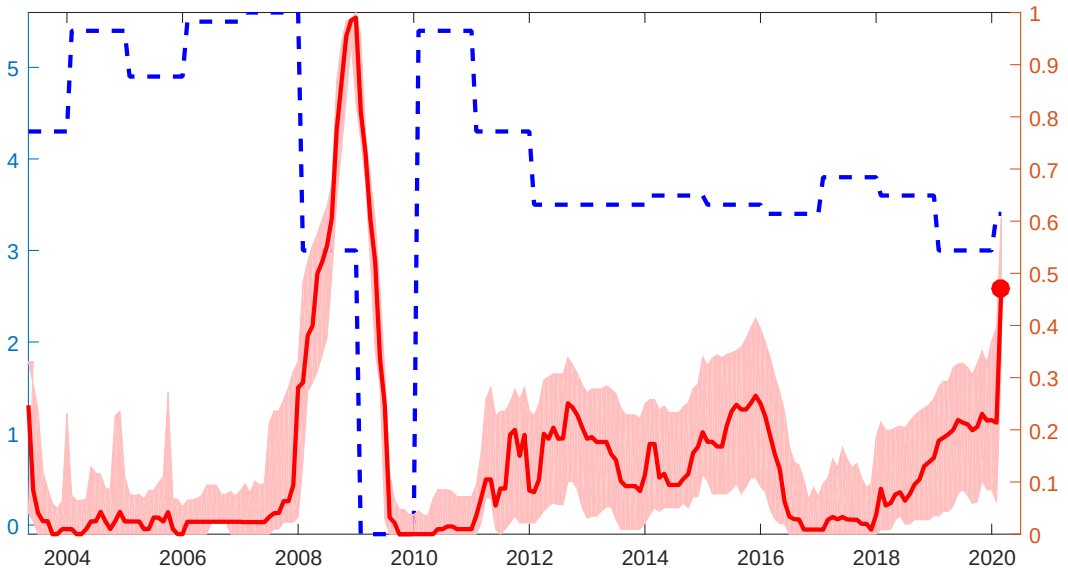

(b) Real-Time Estimates

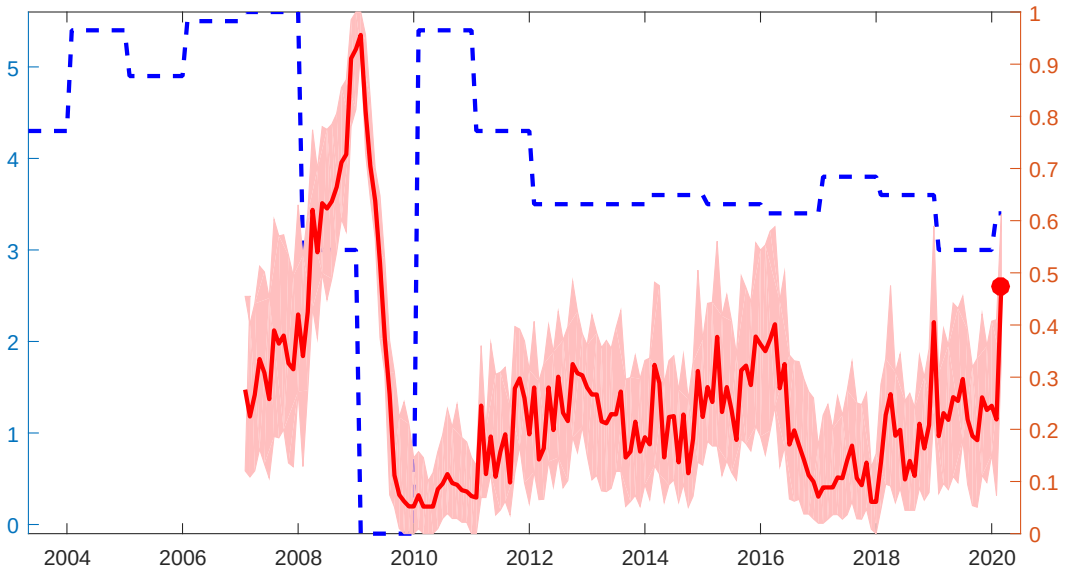

Note: The figure shows the Global Weakness Index, which is constructed as a weighted average of the probabilities of low economic activity regime across countries. The weights are given by the size of the corresponding economies. The red area represents the credible set based on the percentiles 16th and 84th of the posterior distribution. The dashed blue line plots the world real GDP growth based on the estimates provided by the IMF, for comparison purposes. Chart A plots the estimates based on the entire available sample for each world regions. Chart B plots the real-time estimates, which are computed with the available set of information for each world region at the moment of the estimation.

Figure 5: Timeliness of the Global Weakness Index

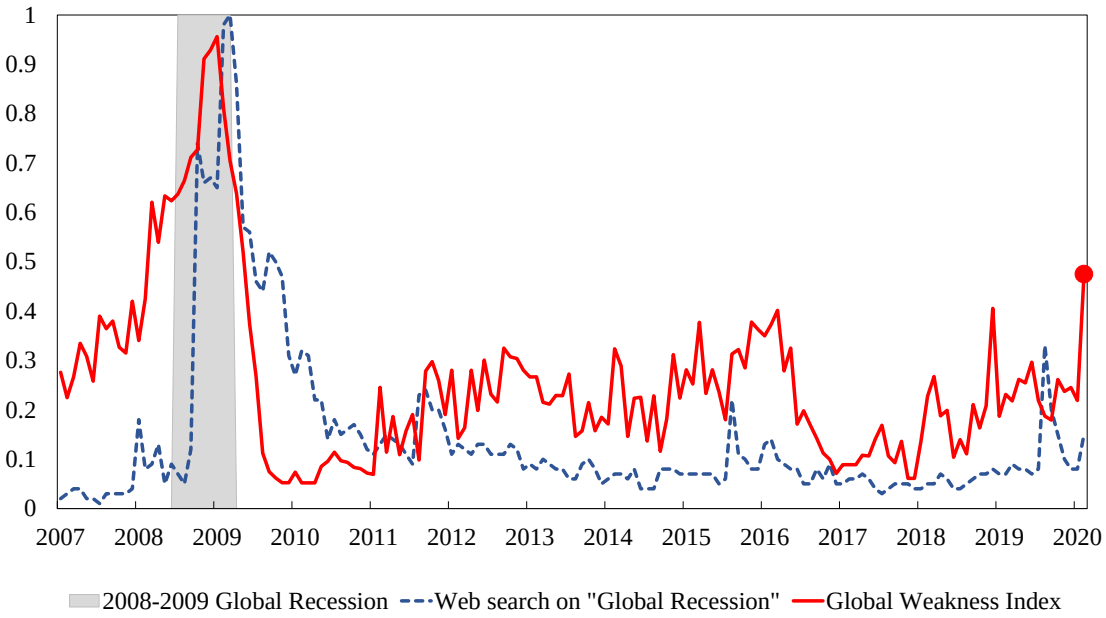

Note: The figure shows the real-time Global Weakness Index (red solid line) and a monthly index numbers that represent web search interest for the term "global recession" (blue dashed line). The web search index is constructed relative to its highest point, with a peak popularity for the term that equals to 1. The information to construct the web search index is obtained from Google Trends. The grey bar represents the period of the last global recession (2008:III-2009:I), as dated in Kose at al. (2020).

Figure 6: Historical Decomposition of Global Weakness

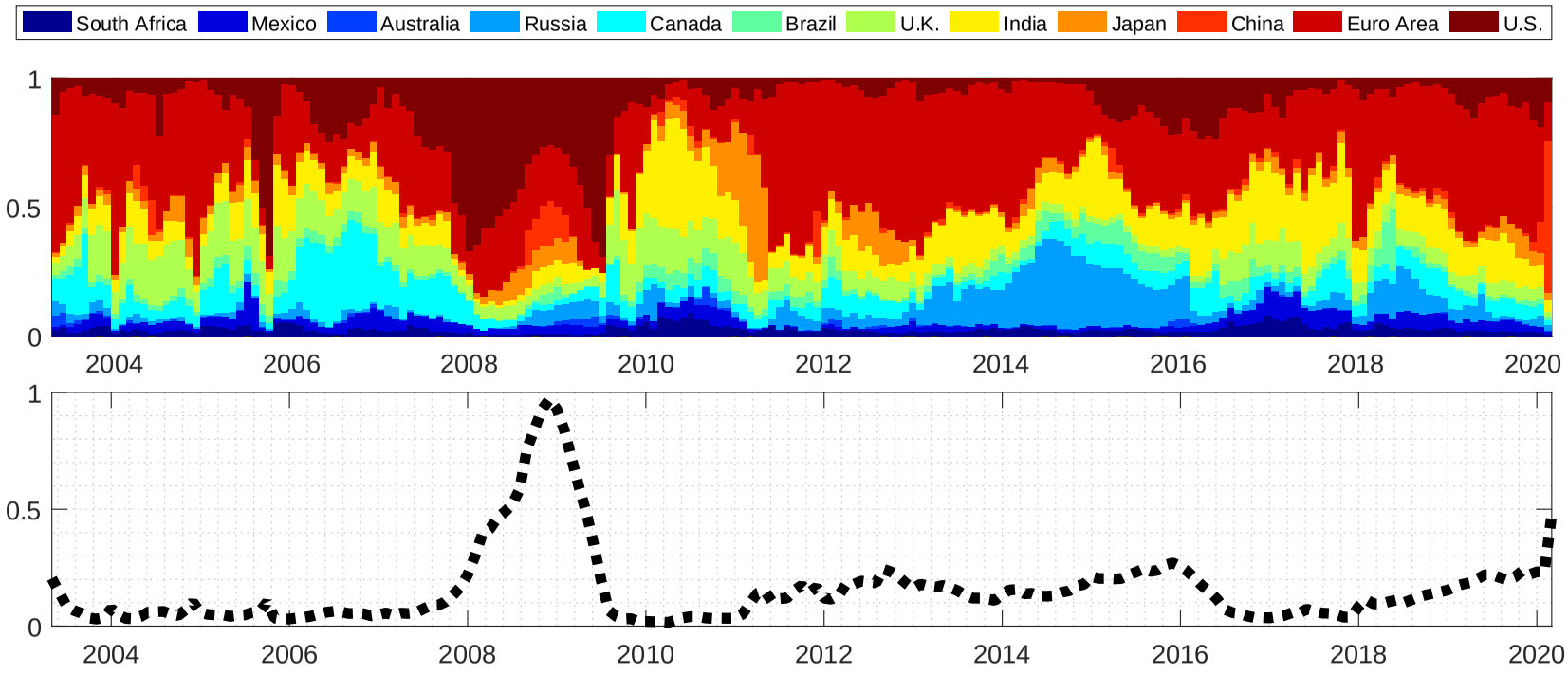

Note: The top chart plots normalized contributions of each economic region to the Global Weakness Index. The contribution of each region, at a given time, is defined as the product between the associated (i) probability of low economic activity, and (ii) the weight of the economy, which is defined by the its relative size in terms of GDP, see Equation (8). The contributions are normalized to sum up to one at every period. The bottom chart plots the full-sample estimates of the Global Weakness Index for reference purposes.

Figure 7: Real-Time Monitoring of Global Risks

(a) 2008M3: The coming of the storm

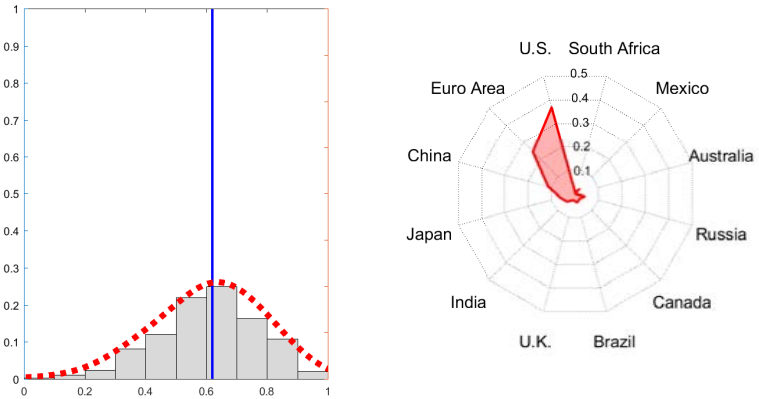

(b) 2009M01: Middle of the last global recession

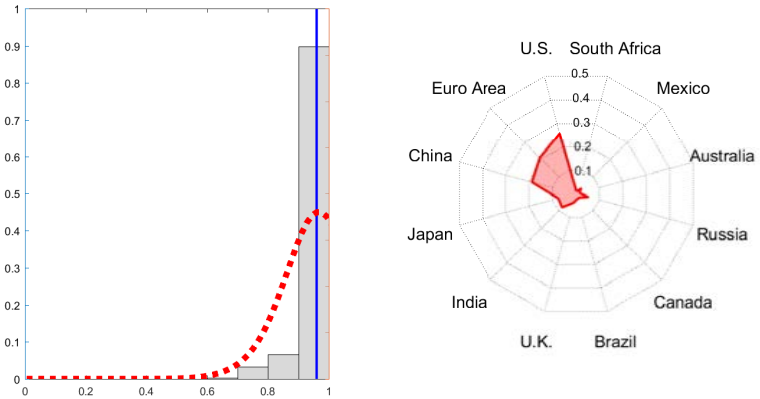

(c) 2009M12: A buoyant global economy

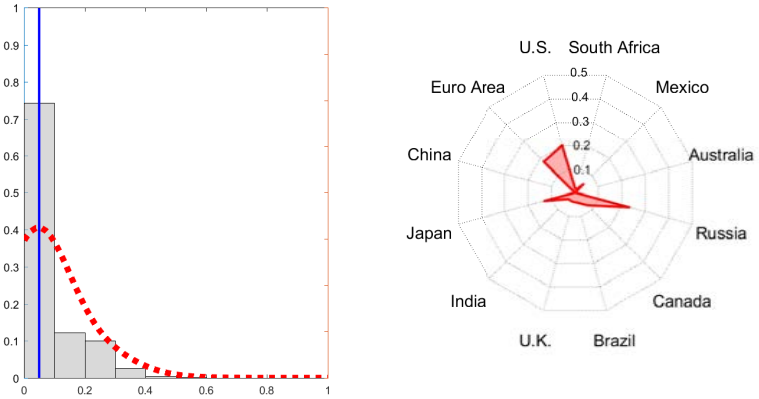

(d) 2020M02: Current situation

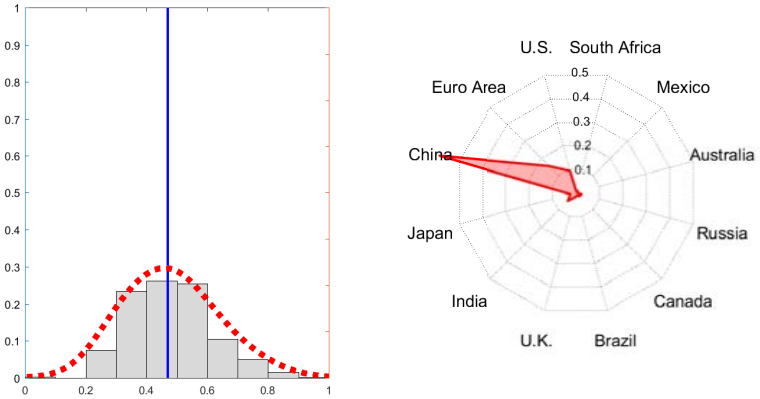

Note: The figure contains four charts associated to different time periods of interest. Each chart contains two sub-charts. The sub-charts on the left provide information on the posterior distribution of the (real-time) Global Weakness Index, where the gray bars show the histograms, red dashed lines indicate the kernel densities, and blue solid lines make reference to the median of the corresponding posterior distributions. The radar sub-charts on the right show information about the relative contribution of each economic region to the Global Weakness Index. The contributions are normalized to sum up to one.

Figure 8: Risk Assessment of Global Weakness

(a) Selected Degrees of Weakness

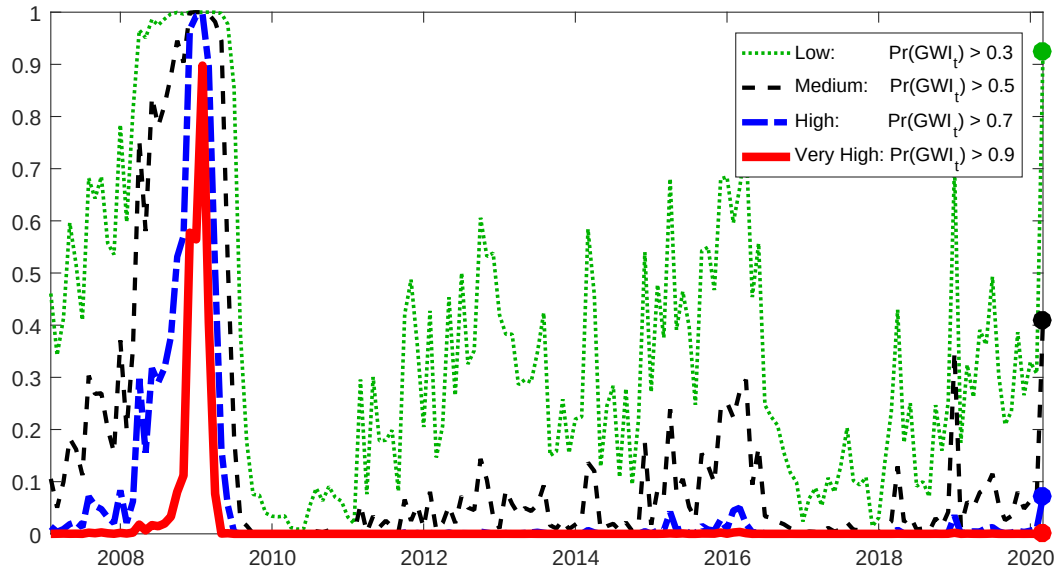

(b) All Degrees of Weakness

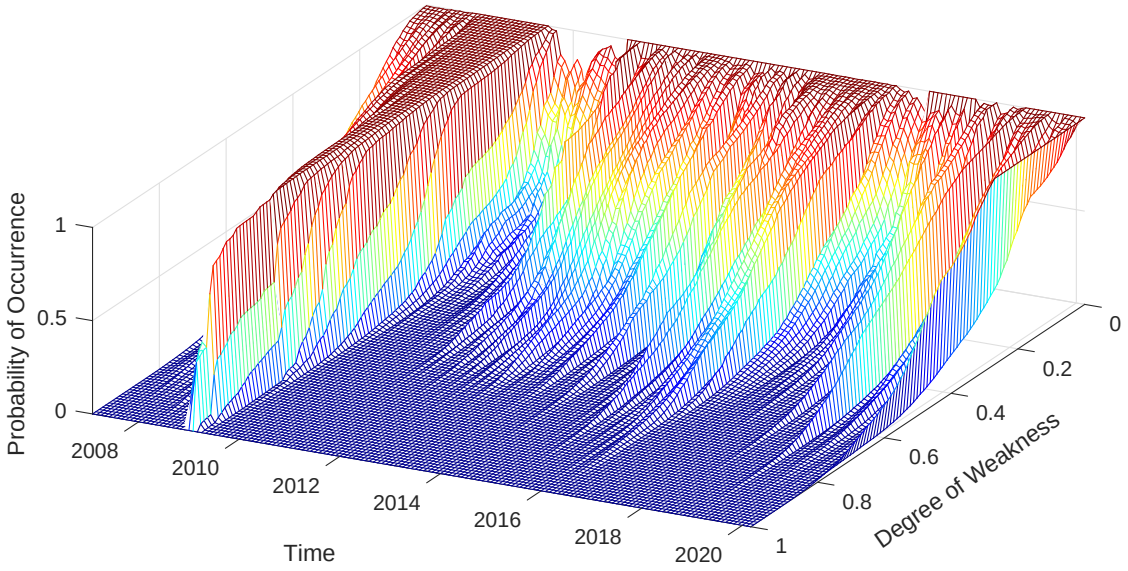

Note: Chart A plots the time-varying probability associated to a scenario in which the GWI reaches values higher than a given threshold. The selected thresholds are 0.3, 0.5, 0.7 and 0.9. Chart B plots the time-varying probability associated to a scenario in which the GWI reaches values higher than a any value between 0 and 1. These probabilities are computed based on the posterior density of the Global Weakness Index.

Figure 9: Risk Assessment of Global Weakness Before and During the Great Recession

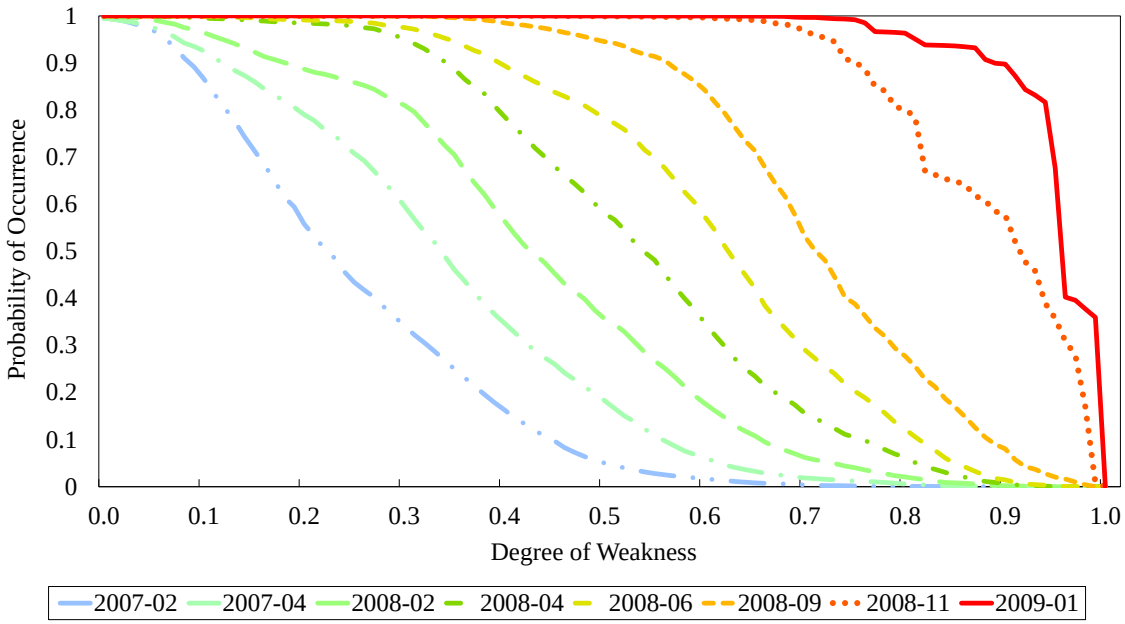

Note: The figure plots the curves that relate level of global weakness with probabilities of occurrence for selected time periods before and during the last global recession. The definition of the selected time periods is shown in the bottom legend.

Table 1: List of variables used for each economic region

ID	*Variable*	*Frequency*	*Sample*
	Australia		
AU1	Real GDP	Quarterly	1997:II – 2019:III
AU2	Industrial production index	Monthly	1997:04 – 2019:08
AU3	Imports of goods and services	Monthly	1997:04 – 2019:12
AU4	Exports of goods and services	Monthly	1997:04 – 2019:12
AU5	Consumer sentiment index	Monthly	1997:04 – 2020:02
	Brazil		
BR1	Real GDP	Quarterly	1996:II – 2019:III
BR2	Industrial Production Index	Monthly	2002:04 – 2019:12
BR3	Total production of vehicles	Monthly	1996:04 – 2020:01
BR4	Retail trade: volume of sales	Monthly	2000:04 – 2019:12
BR5	Merchandise exports	Monthly	1996:04 – 2020:02
	Canada		
CA1	Real GDP	Quarterly	1980:I – 2019:III
CA2	Monthly index of gross domestic product	Monthly	1980:01 – 2019:12
CA3	Index of production of total industry	Monthly	1980:01 – 2019:11
CA4	Exports: value goods in US Dollars	Monthly	1980:01 – 2019:12
CA5	Imports: value goods in US Dollars	Monthly	1980:01 – 2019:12
	China		
CN1	Real GDP	Quarterly	1992:II – 2019:IV
CN2	PMI: Manufacturing (50+=Expansion)	Monthly	2004:05 – 2020:02
CN3	Freight quantity: Imports and Exports (10,000 Metric Tons)	Monthly	2012:02 – 2019:12
CN4	Exports: value goods in US dollars	Monthly	1992:04 – 2019:12
CN5	Imports: value goods in US dollars	Monthly	1992:04 – 2019:12
	Euro Area		
EA1	Real GDP	Quarterly	1995:II – 2019:IV
EA2	Industrial production excluding construction	Monthly	1995:01 – 2019:12
EA3	Intra-euro area exports of goods	Monthly	1999:02 – 2019:11
EA4	Extra-euro area exports of goods	Monthly	1999:02 – 2019:11
EA5	Industrial orders	Monthly	1995:02 – 2020:02
	India		
IN1	Real GDP	Quarterly	1996:III – 2019:III
IN2	Industrial production index: Electricity	Monthly	2005:05 – 2019:12
IN3	Industrial production index excluding construction	Monthly	1996:04 – 2019:12
IN4	Merchandise exports, f.o.b. in US dollars	Monthly	1996:04 – 2020:01
IN5	Merchandise Imports, c.i.f. in US dollars	Monthly	1996:04 – 2020:01
	Japan		
JP1	Real GDP	Quarterly	1993:II – 2019:III
JP2	Industrial production manufacturing index	Monthly	1993:04 – 2020:01
JP3	Construction industry activity index	Monthly	1993:04 – 2019:12
JP4	Exports of goods in Yens	Monthly	1993:04 – 2020:01
JP5	Producer shipment durable consumer goods	Monthly	1993:04 – 2019:12
	Mexico		
MX1	Real GDP	Quarterly	1980:II – 2019:IV
MX2	Industrial production index	Monthly	1980:04 – 2019:12
MX3	Motor vehicle production	Monthly	1983:04 – 2020:01
MX4	Retail sales volume (Goods and Services)	Monthly	1994:04 – 2019:12
MX5	Exports, f.o.b. in US dollars	Monthly	1980:04 – 2020:01
	Russia		
RU1	Real GDP	Quarterly	2003:II – 2019:III
RU2	Imports: value goods for the Russian Federation in US dollars	Monthly	2003:04 – 2019:11
RU3	Exports: value goods for the Russian Federation in US dollars	Monthly	2003:04 – 2019:11
RU4	Industrial Production Index	Monthly	2006:04 – 2020:01
RU5	Passenger Car Sales (Imported Plus Domestic)	Monthly	2006:04 – 2020:01
	South Africa		
SA1	Real GDP	Quarterly	1980:II – 2019:III
SA2	Volume of production (manufacturing)	Monthly	1980:04 – 2019:012
SA3	Merchandixe exports	Monthly	1980:04 – 2020:01
SA4	New vehicules sold	Monthly	1980:04 – 2019:12
SA5	Electricity production	Monthly	1985:02 – 2019:12
	United Kingdom		
UK1	Real GDP	Quarterly	1980:II – 2019:IV
UK2	Index of industrial production	Monthly	1980:04 – 2019:12
UK3	Exports: value goods in Pounds	Monthly	1980:04 – 2019:12
UK4	Passenger Car Registration	Monthly	1980:04 – 2020:01
UK5	MFG Order Books	Monthly	1980:04 – 2020:02
	United States		
US1	Real GDP	Quarterly	1947:II – 2019:IV
US2	Industrial production index	Monthly	1947:04 – 2020:01
US3	All employees, total nonfarm	Monthly	1947:04 – 2020:01
US4	Real personal income excluding current transfer receipts	Monthly	1959:04 – 2020:01
US5	Real manufacturing and trade industries sales	Monthly	1967:04 – 2019:12

Note: The table reports the list of variables used in the models fitted to each economic region, along with frequency and coverage period.

A Online Appendix

A.1 Full specification of the model

The common factor f_t affects all the observed variables; it evolves according to the following rule:

$$f_t = \mu_0(1 - s_t) + \mu_1 s_t + s_t x_t + e_{f,t}, \quad e_{f,t} \sim \mathcal{N}(0, \sigma_f^2). \tag{A.1}$$

The indicator $s_t \in \{0, 1\}$ equals one whenever there is an abnormal episode; it is a two-state Markov-switching process whose evolution is summarized by $p = \Pr(s_t = 1|s_{t-1} = 1)$ and $q = \Pr(s_t = 0|s_{t-1} = 0)$. In case of an abnormal episode ($s_t = 1$), the common factor is augmented by an unobserved variable x_t, which evolves as follows:

$$x_t = s_t x_{t-1} + (1 - s_t)v_t, \quad v_t \sim \mathcal{N}(0, \sigma_v^2). \tag{A.2}$$

Whenever there is an abnormal episode, the common factor is augmented by x_t, which takes a random value at the beginning of the episode and then remains constant for the duration of the episode.

Each monthly variable is assumed to be a combination of the common factor f_t and an individual component $u_{i,t}$:

$$y_{i,t}^m = \gamma_i f_t + u_{i,t}. \tag{A.3}$$

Each individual component is assumed to have P lags:

$$u_{i,t} = \psi_{i,1} u_{i,t-1} + ... + \psi_{i,P} u_{i,t-P} + e_{i,t}, \quad e_{i,t} \sim \mathcal{N}(0, \sigma_i^2). \tag{A.4}$$

In addition, following Mariano and Murasawa (2003), the growth rate of a variable observed with quarterly frequency (such as the GDP) can be expressed as a combination of its monthly unobserved growth rates as follows:

$$y_{j,t}^q = \frac{1}{3} y_{j,t}^m + \frac{2}{3} y_{j,t-1}^m + y_{j,t-2}^m + \frac{2}{3} y_{j,t-3}^m + \frac{1}{3} y_{j,t-4}^m. \tag{A.5}$$

In turn, the monthly growth rates have the same decomposition as described in equation (A.3), so that we can express each quarterly growth rate as a combination of the common factor and

the individual component, as follows:

$$y^q_{j,t} = \frac{1}{3}\gamma_j f_t + \frac{2}{3}\gamma_j f_{t-1} + \gamma_j f_{t-2} + \frac{2}{3}\gamma_j f_{t-3} + \frac{1}{3}\gamma_j f_{t-4} + \\ + \frac{1}{3}u_{j,t} + \frac{2}{3}u_{j,t-1} + u_{j,t-2} + \frac{2}{3}u_{j,t-3} + \frac{1}{3}u_{j,t-4}. \quad \text{(A.6)}$$

As for the individual components of the quarterly series, they have the same structure as those described by equation (A.4) for the monthly series.

Let there be Q quarterly observable variables and M monthly observable variables, and let us summarize them by vector $y_t = [y^q_{1,t}, ..., y^q_{Q,t}, y^m_{Q+1,t}, ..., y^m_{Q+M,t}]'$. To summarize equations (A.3)–(A.6) into an observation equation, we need to define the vector of unobserved states $z_t = [f_t, ..., f_{t-4}, u_{1,t}, ..., u_{1,t-4}, ..., u_{Q,t}, ..., u_{Q,t-4}, u_{Q+1,t}, ..., u_{Q+1,t-P+1}, ..., u_{Q+M,t}, ..., u_{Q+M,t-P+1}]'$. As we can see, the vector z_t combines the common factor with lags up to 4 and individual components of the quarterly variables with lags up to 4 in order to account for the representation of quarterly variables according to equation (A.6); it also includes individual components of the monthly variables with lags up to $P-1$.[14] Then, assuming that all the variables are observed in period t, we can formulate the observation equation:

$$y_t = \mathbf{H}z_t + \eta_t, \quad \eta_t \sim \mathcal{N}(0, \mathbf{R}) \quad \text{(A.7)}$$

where η_t is a vector of measurement errors, and $(Q+M) \times (5+5Q+PM)$ matrix $\mathbf{H}$ is the following:

$$\mathbf{H} = \begin{bmatrix} \gamma_1 \times \mathbf{H}_Q & \mathbf{H}_Q & \cdots & 0 & 0 & \cdots & 0 \\ \vdots & \vdots & \ddots & \vdots & \vdots & \ddots & \vdots \\ \gamma_Q \times \mathbf{H}_Q & 0 & \cdots & \mathbf{H}_Q & 0 & \cdots & 0 \\ \gamma_{Q+1} \times \mathbf{H}^5_M & 0 & \cdots & 0 & \mathbf{H}^P_M & \cdots & 0 \\ \vdots & \vdots & \ddots & \vdots & \vdots & \ddots & \vdots \\ \gamma_{Q+M} \times \mathbf{H}^5_M & 0 & \cdots & 0 & 0 & \cdots & \mathbf{H}^P_M \end{bmatrix}, \quad \text{(A.8)}$$

$$\mathbf{H}_Q = \begin{bmatrix} \frac{1}{3} & \frac{2}{3} & 1 & \frac{2}{3} & \frac{1}{3} \end{bmatrix}, \quad \mathbf{H}^5_M = \begin{bmatrix} 1 & 0 & 0 & 0 & 0 \end{bmatrix}, \quad \mathbf{H}^P_M = \begin{bmatrix} 1 & 0 & ... & 0 \end{bmatrix}.$$

[14] Because the lags for quarterly variables' individual components are capped at 4, this specification effectively restricts P to be no greater then 5. This restriction can easily be relaxed.

Note that the size of the matrix $\mathbf{H}_M^P$ is $1 \times P$, and the only non-zero element is the first one. More generally, in periods when some of the observations are missing, the observation equation can be cast without the rows that correspond to the missing observations:

$$y_t^* = \mathbf{H}_t z_t + \eta_t^*, \quad \eta_t^* \sim \mathcal{N}(0, \mathbf{R}_t) \tag{A.9}$$

where $\mathbf{H}_t$ is obtained by taking $\mathbf{H}$ and eliminating the columns that correspond to the missing variables, and the matrix $\mathbf{R}_t$ is obtained by eliminating the corresponding rows and columns from matrix $\mathbf{R}$.

Next, let us define the dynamics of the unobserved state z_t:

$$z_t = \begin{bmatrix} s_t\mu_0 + (1-s_t)\mu_1 + s_t x_t \\ 0 \\ \vdots \\ 0 \end{bmatrix} + \mathbf{F} z_{t-1} + \varepsilon_t, \quad \varepsilon_t \sim \mathcal{N}(0, \mathbf{Q}), \tag{A.10}$$

In this equation, $\mathbf{F}$ is a $(5 + 5Q + PM) \times (5 + 5Q + PM)$ matrix, which can be compactly expressed as follows:

$$\mathbf{F} = \begin{bmatrix} \mathbf{F}_0 & \mathbf{0} & \cdots & \mathbf{0} \\ \mathbf{0} & \mathbf{\Psi}_1 & \cdots & \mathbf{0} \\ \vdots & \vdots & \ddots & \vdots \\ \mathbf{0} & \mathbf{0} & \cdots & \mathbf{\Psi}_{M+Q} \end{bmatrix}, \quad \text{where} \quad \mathbf{F}_0 = \begin{bmatrix} 0 & 0 & 0 & 0 & 0 \\ 1 & 0 & 0 & 0 & 0 \\ 0 & 1 & 0 & 0 & 0 \\ 0 & 0 & 1 & 0 & 0 \\ 0 & 0 & 0 & 1 & 0 \end{bmatrix}.$$

As for the matrix $\mathbf{\Psi}_i$, it is a 5×5 matrix for quarterly series ($i = 1, ..., Q$), since there are four lags of monthly individual components for each quarterly series in the state vector z_t:

$$\mathbf{\Psi}_i = \begin{bmatrix} \psi_{i,1} & \psi_{i,2} & \psi_{i,3} & \psi_{i,4} & \psi_{i,5} \\ 1 & 0 & 0 & 0 & 0 \\ 0 & 1 & 0 & 0 & 0 \\ 0 & 0 & 1 & 0 & 0 \\ 0 & 0 & 0 & 1 & 0 \end{bmatrix}$$

However, the coefficients $\psi_{i,p}$ are non-zero only for $p < P$, where P is the number of specified lags.[15] In case of monthly series ($i = Q+1, ..., Q+M$), the matrix $\mathbf{\Psi}_i$ is $P \times P$.

Vector ε_t contains shocks to the common factor and each individual component:

$$\varepsilon_t = \Big[[e_{f,t}, 0, 0, 0, 0],\ [e_{1,t}, 0, 0, 0, 0],\ ...,\ [e_{M+Q,t}, 0, 0, 0, 0]\Big]'. \tag{A.11}$$

Correspondingly, the matrix Q is a diagonal matrix, such that

$$diag(\mathbf{Q}) = \Big([\sigma_f^2, 0, 0, 0, 0],\ [\sigma_1^2, 0, 0, 0, 0],\ ...,\ [\sigma_{M+Q}^2, 0, 0, 0, 0]\Big). \tag{A.12}$$

Note that the dynamics equation (A.10) contains an extra vector that depends on the state indicator s_t and the latent variable x_t—this does not complicate the application of the Kalman filter, since the Bayesian estimation that we use takes turns to simulate $\{z_t\}_{t=1}^T$, then $\{x_t\}_{t=1}^T$, and then $\{s_t\}_{t=1}^T$. For example, during the step that simulates $\{z_t\}_{t=0}^T$, the value $s_t\mu_0+(1-s_t)\mu_1+s_t x_t$ is fixed and therefore treated as a constant.

Equations (A.2), (A.7)–(A.12) summarize the model that we estimate, and the model is summarized by parameter vector θ:

$$\theta = \Big\{p, q, \mu_0, \mu_1, \sigma_v, \sigma_f, \gamma_1, ..., \gamma_{Q+M}, \{\psi_{1,1}, ..., \psi_{1,P}\}, ..., \{\psi_{Q+M,1}, ..., \psi_{Q+M,P}\}, \sigma_1, ..., \sigma_{Q+M}\Big\}.$$

A.2 Bayesian estimation

Let $Y = \{y_t\}_{t=0}^T$ be the observed data that consists of quarterly and monthly growth rates normalized by their standard deviations. Let $Z^i = \{z_t^i\}_{t=0}^T$, $X^i = \{X_t^i\}_{t=0}^T$, and $S^i = \{S_t^i\}_{t=0}^T$ be the i-th simulation of the unobserved variables, and let θ^i be the i-th simulation of the parameter vector. The Bayesian procedure follows (Carter and Kohn, 1994) algorithm, iterating upon Z, X, S, and θ.

1. Given Y, S^i, X^i, and θ^i, and using the dynamics equation (A.10) and the measurement equation (A.7), simulate Z^{i+1} using Carter and Kohn (1994):

   a. Initialize $z_{1|0}$ as a vector with the first element equal to $\mu_0 s_1^i + \mu_1(1 - s_1^i) + s_1^i x_1^i$ and the remaining elements equal to zero, and $P_{1|0} = I$.

[15] We restrict the individual components for the quarterly series to be white noises in the model, so that the first row of $\mathbf{\Psi}_i$ is zero for $i \leq Q$.

b. Run standard Kalman filter to evaluate $\{z_{t|t}, P_{t|t}\}_{t=0}^{T}$:

- Account for missing observations in vector y_t: define y_t^* by eliminating the missing observations, define H_t^* by eliminating the rows that correspond to the missing observations, and define R_t^* by eliminating the rows and the columns that correspond to the missing observations.
- For $t = 1, ..., T$, compute the following:

  - Forecast:

    $$\Omega_{t|t} = H_t^* P_{t|t-1}(H_t^*)' + R_t^*;$$

    $$\nu_t = y_t - H_t^* z_{t|t-1};$$

    Update:

    $$z_{t|t} = z_{t|t-1} + P_{t|t-1}(H_t^*)'(\Omega_{t|t-1})^{-1}\nu_t;$$

    $$P_{t|t} = P_{t|t-1} - P_{t|t-1}(H_t^*)'(\Omega_{t|t-1})^{-1}H_t^* P_{t|t-1};$$

    Prediction:

    $$z_{t+1|t} = F z_{t|t} + \left[\; s_{t+1}^i(\mu_0 + x_{t+1}^i) + (1 - s_{t+1}^i)\mu_1, \; 0, \; ..., \; 0 \; \right]';$$

    $$P_{t+1|t} = F P_{t|t} F' + Q.$$

c. Using the output from the Kalman filter, run the smoothing filter backwards in order to obtain $\{z_{t|T}, P_{t|T}\}_{t=0}^{T}$:

- Account for the fact that in the dynamics equation (A.10), shocks in vector ε_t do not affect all the state variables contemporaneously, so that the matrix Q is singular, and $\Omega_{t|t-1}$ is potentially non-invertible. Define $\hat{z}_t$ by eliminating the rows that correspond to zero elements in the vector ε_t: according to equation (A.11), this means discarding all elements but the first, the fifth, etc. Similarly, define $\hat{F}$ by eliminating the corresponding rows, and define $\hat{Q}$ by eliminating the corresponding rows and columns.
- For $t = T$, Kalman filter has already delivered $z_{t|t} = z_{t|T}$ and $P_{t|t} = P_{t|T}$ in step (b). We can use this information to simulate $z_T^{i+1} \sim \mathcal{N}(z_{T|T}, P_{T|T})$, and then eliminate part of its elements, as described above, to get $\hat{z}_T^{i+1}$.

- Going with t backwards from $T-1$ to 1, compute the following:

  - Forecast and forecast error:

    $\hat{\Omega}_{t+1|t} = \hat{F} P_{t|t} (\hat{F})' + \hat{Q}$;

    $\hat{z}_{t+1|t} = \hat{F} z_{t|t} + \left[\, s^i_{t+1}(\mu_0 + x^i_{t+1}) + (1 - s^i_{t+1})\mu_1, \; 0, \; ..., \; 0 \, \right]'$;

    $\nu_{t+1} = \hat{z}^{i+1}_{t+1} - \hat{z}_{t+1|t}$;

  - Use the information from $t+1$ to update the estimates for t:

    $z_{t|T} = z_{t|t+1} = z_{t|t} + P_{t|t}(\hat{F})'(\hat{\Omega}_{t+1|t})^{-1}\nu_{t+1}$;

    $P_{t|T} = P_{t|t+1} = P_{t|t} - P_{t|t}(\hat{F})'(\hat{\Omega}_{t+1|t})^{-1}\hat{F}P_{t|t}$;

  - Use the obtained information to randomize $z^{i+1}_t \sim \mathcal{N}(z_{t|T}, P_{t|T})$;

  - Eliminate, as described above, elements of z^{i+1}_t to obtain $\hat{z}^{i+1}_t$.

2. Given Z^{i+1}, X^i, and θ^i, operate upon the equation (A.1) to simulate indicators S^{i+1} following Carter and Kohn (1994):

   a. Going forwards, for $t = 1, .., T$, compute $P_t(s_t = 0)$:

   - The initial unconditional probability of normal state is

     $$P_0(s_0 = 0) = \frac{1-q}{2-q-p}.$$

   - For $t = 1, ..., T$, first compute

     $$P_{t-1}(s_t = 0) = P_{t-1}(s_{t-1} = 0) \times p + \big(1 - P_{t-1}(s_{t-1} = 0)\big) \times (1-q);$$

     and observe that

     $$f_t | s_t = 0 \sim \mathcal{N}(\mu_0, \sigma^2_e),$$
     $$f_t | s_t = 1 \sim \mathcal{N}(\mu_1 + x^i_t, \sigma^2_e).$$

     Then,

     $$P_t(s_t = 0) = \frac{P_{t-1}(s_t = 0)\phi\left(\frac{f_t - \mu_0}{\sigma_e}\right)}{P_{t-1}(s_t = 0)\phi\left(\frac{f_t - \mu_0}{\sigma_e}\right) + \big(1 - P_{t-1}(s_t = 0)\big)\phi\left(\frac{f_t - \mu_1 - x^i_t}{\sigma_e}\right)}.$$

b. Going backwards for $t = T, ..., 1$, compute $P_{t+1}(s_t = 0) = P_T(s_t = 0)$ and simulate the state indicators using these probabilities:

- For the last period, we have $P_T(s_T = 0)$ from step (a). Simulate s_T^{i+1} using this probability.
- For $t = T - 1, ..., 1$, compute the probabilities as follows:

$$s_{t+1}^{i+1} = 0 \Rightarrow P_{t+1}(s_t = 0) = \frac{P_t(s_t = 0) \times p}{P_t(s_t = 0) \times p + \big(1 - P_t(s_t = 0)\big) \times (1 - q)};$$
$$s_{t+1}^{i+1} = 1 \Rightarrow P_{t+1}(s_t = 0) = \frac{P_t(s_t = 0) \times (1 - p)}{P_t(s_t = 0) \times (1 - p) + \big(1 - P_t(s_t = 0)\big) \times q}.$$

Then, since $P_{t+1}(s_t = 0) = P_T(s_t = 0)$, use this probability to simulate s_t^{i+1}

3. Given, S^{i+1}, θ^i, and Z^{i+1}, simlulate X^{i+1} using Carter and Kohn (1994). It is the same routine as in step 1, except that now, the dynamics of the unobserved state are given by equation (A.2), and the "measurement" equation is equation (A.1) for the common factor, in which all the elements except for x_t are fixed. A major simplification is that the common factor values are known for all periods $t = 1, ..., T$, and both the common factor f_t and the latent variable x_t are one-dimensional, so there is no need to reduce the dimensionality of the equations to account for missing variables or singularity.

4. Finally, given Y, S^{i+1}, Z^{i+1}, and X^{i+1}, compute θ^{i+1} using standard pior distributions:

a. The prior distribution for σ_v^2, the variance of the shock affecting the unobserved process x_t, is inverse-gamma: $\sigma_v^2 \sim \mathcal{IG}(a, b)$. Then, the posterior is also inverse-gamma, $\mathcal{IG}(\bar{a}, \bar{b})$, such that

$$\bar{a} = a + \frac{T}{2}, \quad \bar{b} = b + \frac{\sum (x_t^i - s_t^i x_{t-1}^i)^2}{2}.$$

We sample $(\sigma_v^{i+1})^2$ from this posterior.

b. Similarly, the prior distribution for σ_e^2, the variance of the shock affecting the common factor f_t, is inverse-gamma: $\sigma_e^2 \sim \mathcal{IG}(a, b)$. Then, the posterior is also inverse-gamma, $\mathcal{IG}(\bar{a}, \bar{b})$, such that

$$\bar{a} = a + \frac{T}{2}, \quad \bar{b} = \frac{1}{b + \sum \left(f_t^i - s_t^i(\mu_1^i + x_{t-1}^i) - (1 - s_t^i)\mu_0^i\right)^2 / 2}.$$

We sample $(\sigma_e^{i+1})^2$ from this posterior.

c. The prior distribution for μ_0 and μ_1 is normal:

$$\begin{bmatrix} \mu_0 \\ \mu_1 \end{bmatrix} \sim \mathcal{N}(a, V).$$

Define $Y^* = \{y_t^*\}$, such that $y_t^* = f_t^i - s_t^i \times x_t^i$, and $X^* = [\mathbf{1} - S^i, S^i]$. Then, the posterior distribution is also normal, $\mathcal{N}(\bar{a}, \bar{V})$, such that

$$\bar{V} = \left(V^{-1} + (X^*)'X^*\right)^{-1};$$
$$\bar{a} = \bar{V}\left(V^{-1}a + (X^*)'Y^*\right).$$

The regime-specific means μ_0^{i+1} and μ_1^{i+1} are simulated from this posterior.

d. In our specifications, we have worked with only one quarterly variable, GDP growth. We *fix* the common-factor loading γ_1 for the quarterly GDP growth to be equal to one for identification purposes—this assumption amounts to scaling the common factor. Then, the factor loadings for the monthly variables are interpreted as relative to the unit loading for the GDP growth. In the prior, a factor loading γ_j of a monthly indicator $j = 1, ..., M$ is normally distributed: $\gamma_j \sim \mathcal{N}(a, V)$. Then, define $\tilde{y}_{j,t}$ and $\tilde{f}_{j,t}$ as follows:

$$\tilde{y}_{j,t} = y_{j,t} - \psi_{j,1}^i y_{j,t-1} - ... - \psi_{j,P}^i y_{j,t-P};$$
$$\tilde{f}_{j,t}^i = f_t^i - \psi_{j,1}^i f_{t-1}^i - ... - \psi_{j,P}^i f_{t-P}^i.$$

We can use these definitions together with equations (A.3) and (A.4) to derive the following expression:

$$\tilde{y}_{j,t} = \gamma_j \tilde{f}_{j,t}^i + e_{j,t}, \quad e_{j,t} \sim \mathcal{N}(0, \sigma_j^2).$$

Using this expression, we can find the posterior for the factor loading to be normal

as well: $\gamma_j \sim \mathcal{N}(\bar{a}_j, \bar{V}_j)$, such that

$$\bar{V}_j = \left(V^{-1} + (\tilde{X}_j)'\tilde{X}_j\right)^{-1};$$
$$\bar{a}_j = \bar{V}\left(V^{-1}a + (\tilde{X}_j)'\tilde{Y}_j\right),$$

where $\tilde{X}_j$ and $\tilde{Y}_j$ are vectors with elements $\{\tilde{f}_{j,t}\}$ and $\{\tilde{y}_{j,t}\}$ defined above. Factor loadings $\{\gamma_j^{i+1}\}$ are simulated from these posteriors.

e. We assume that the individual component of the only quarterly variable in our model is a white noise, which makes it simpler to compute the posterior, due to the monthly missing observations in a variable at the quarterly frequency: for the individual component of GDP growth, equation (A.4) reduces to

$$u_{1,t} = e_{1,t}, \quad e_{1,t} \sim \mathcal{N}(0, \sigma_1^2).$$

Then, we specify the inverse-gamma prior $\sigma_1^2 \sim \mathcal{IG}(a, b)$, which conjugates with the inverse-gamma posterior $\mathcal{IG}(\bar{a}, \bar{b})$, such that

$$\bar{a} = a + \frac{T}{2}, \quad \frac{1}{b + \sum (y_{1,t}^i)^2/2}.$$

The variance $(\sigma_1^{i+1})^2$ is simulated from this posterior.

f. Define $Y_j = (y_{j,1}, ..., y_{j,T})$ to be the vector collecting the observations of a monthly variable j. Let X_j be the $T \times P$ matrix recording the P lags of the variable $y_{j,t}$. For the AR coefficients of each monthly variable's individual component, $\psi_j = (\psi_{j,1}, ..., \psi_{j,P})'$, we assume the same normal prior: $\psi_j \sim \mathcal{N}(a, V)$. Then, the posterior is also normal, $\mathcal{N}(\bar{a}_j, \bar{V}_j)$, but different for each j, such that

$$\bar{V}_j = \left(V^{-1}a + \frac{X_j'X_j}{(\sigma_j^i)^2}\right)^{-1};$$
$$\bar{a}_j = \bar{V}_j\left(V^{-1}a + \frac{X_j'Y_j}{(\sigma_j^i)^2}\right)$$

We simulate ψ_j^{i+1} from this posterior. Finally, to simulate σ_j^{i+1}, we assume inverse-

gamma prior: for each j, $\sigma_j^2 \sim \mathcal{IG}(a, b)$. Let Ψ_j^{i+1} be the following $P \times P$ matrix:

$$\Psi_j^{i+1} = \begin{bmatrix} \psi_{j,1}^{i+1} & \cdots & \psi_{j,P-1}^{i+1} & \psi_{j,P}^{i+1} \\ 1 & \cdots & 0 & 0 \\ \vdots & \ddots & \vdots & \vdots \\ 0 & \cdots & 1 & 0 \end{bmatrix}$$

Then, we can express the posterior of σ_j^2 as inverse-gamma distribution as well, $\mathcal{IG}(\bar{a}, \bar{b})$, such that

$$\bar{a} = a + \frac{T}{2}; \quad \bar{b} = \left(b + \frac{(Y_j - X_j \Psi_j^{i+1})'(Y_j - X_j \Psi_j^{i+1})}{2} \right)^{-1}.$$

We simulate AR coefficients $\{\psi_j^{i+1}\}$ from these posteriors.

Figure 10: Euro Area

(a) Probability of low economic activity regime: Constant mean model

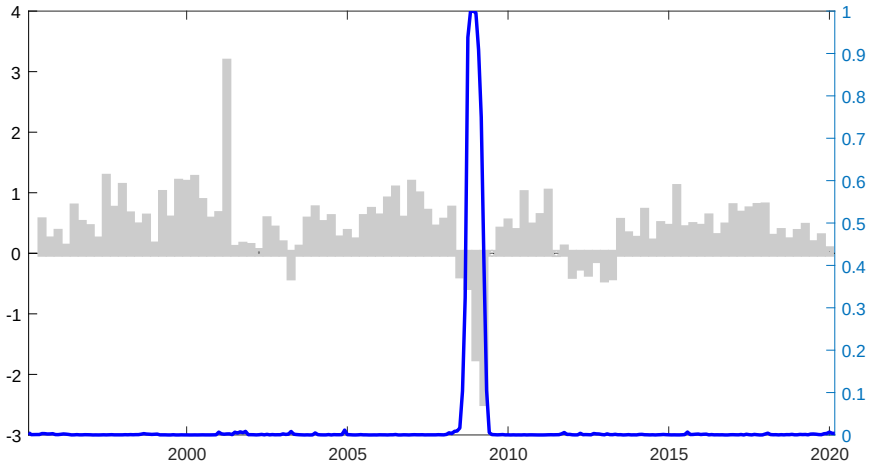

(b) Probability of low economic activity regime: Time-varying mean model

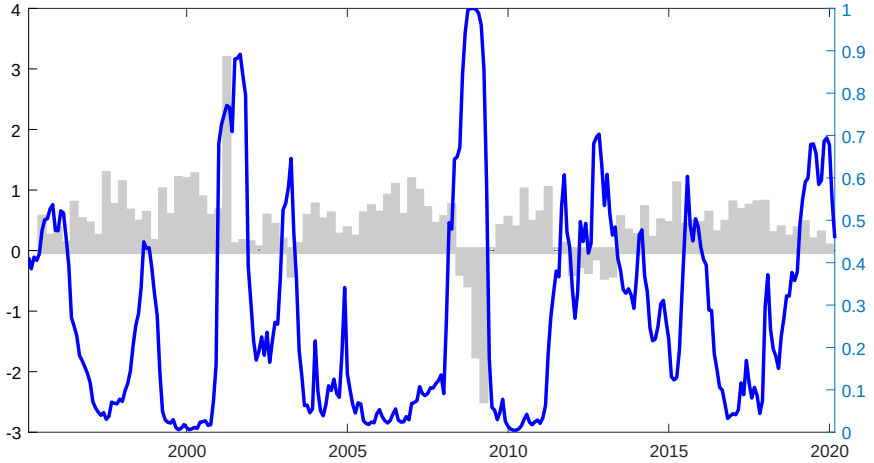

Note: The blue solid line (right axis) plots the monthly probability of low real activity regime, $Pr(s_t = 1)$, for the corresponding model, and the grey bars (left axis) denote the real GDP quarterly growth.

Figure 11: Australia

(a) Probability of low economic activity regime: Constant mean model

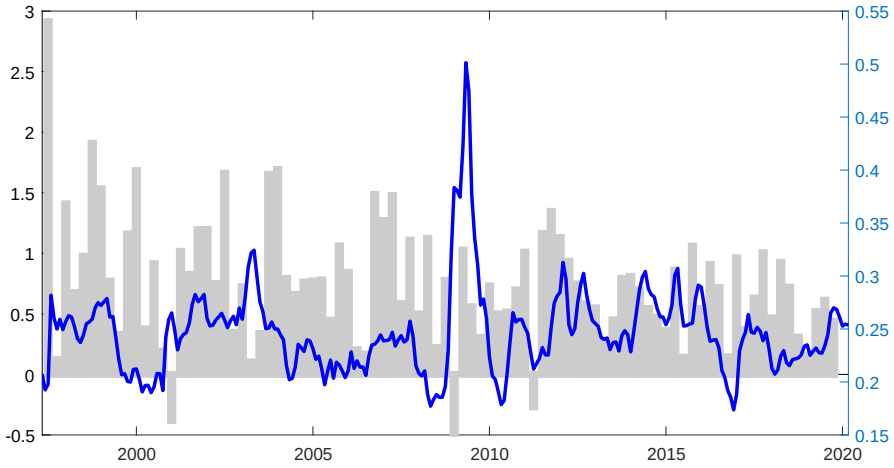

(b) Probability of low economic activity regime: Time-varying mean model

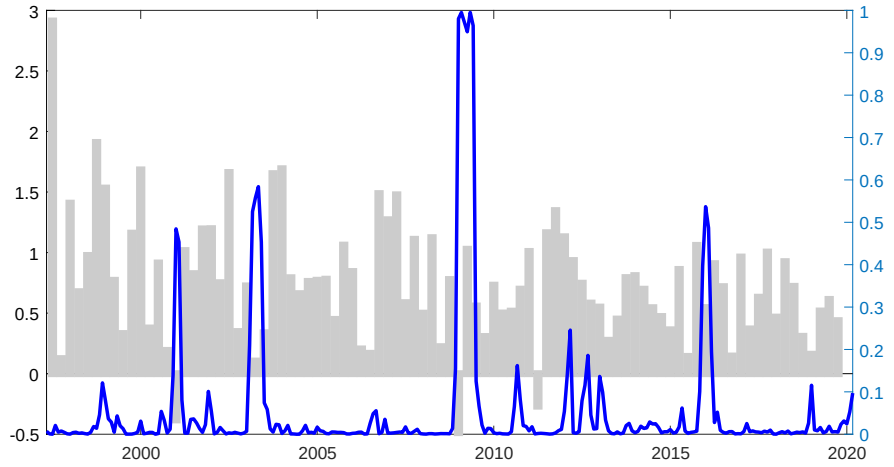

Note: The blue solid line (right axis) plots the monthly probability of low real activity regime, $Pr(s_t = 1)$, for the corresponding model, and the grey bars (left axis) denote the real GDP quarterly growth.

Figure 12: Canada

(a) Probability of low economic activity regime: Constant mean model

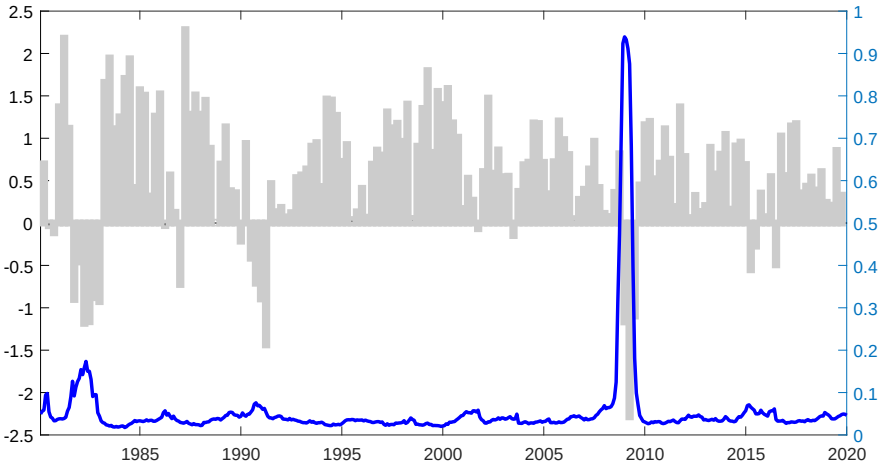

(b) Probability of low economic activity regime: Time-varying mean model

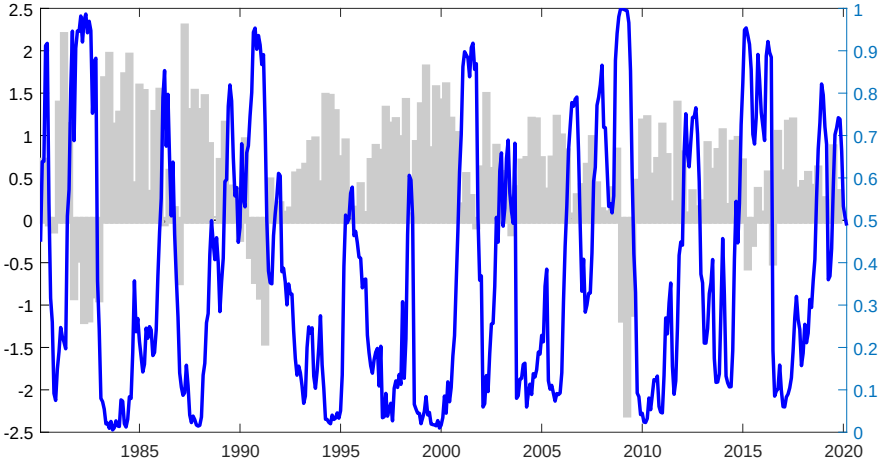

Note: The blue solid line (right axis) plots the monthly probability of low real activity regime, $Pr(s_t = 1)$, for the corresponding model, and the grey bars (left axis) denote the real GDP quarterly growth.

Figure 13: Japan

(a) Probability of low economic activity regime: Constant mean model

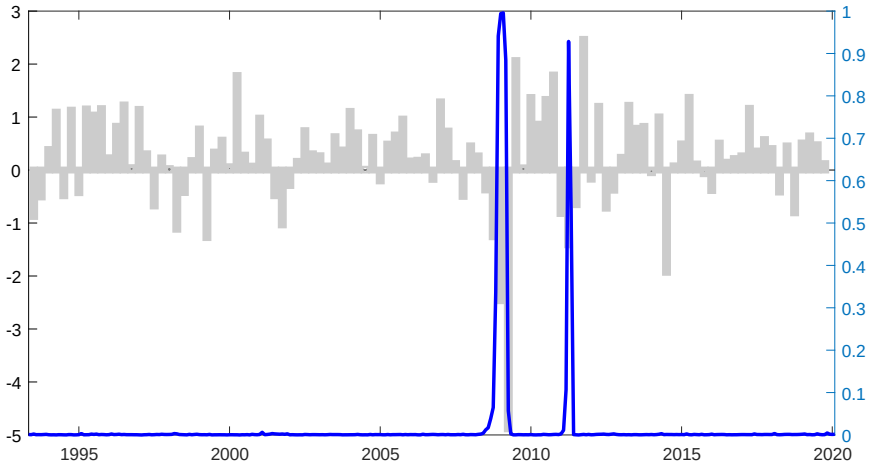

(b) Probability of low economic activity regime: Time-varying mean model

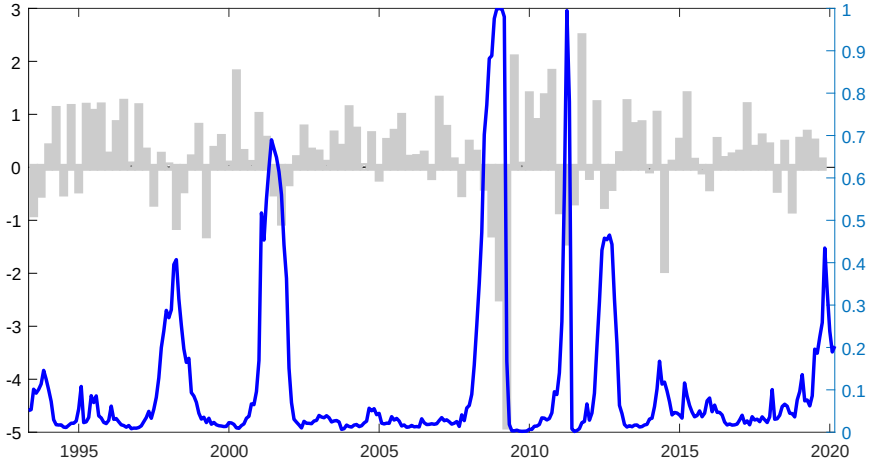

Note: The blue solid line (right axis) plots the monthly probability of low real activity regime, $Pr(s_t = 1)$, for the corresponding model, and the grey bars (left axis) denote the real GDP quarterly growth.

Figure 14: United Kingdom

(a) Probability of low economic activity regime: Constant mean model

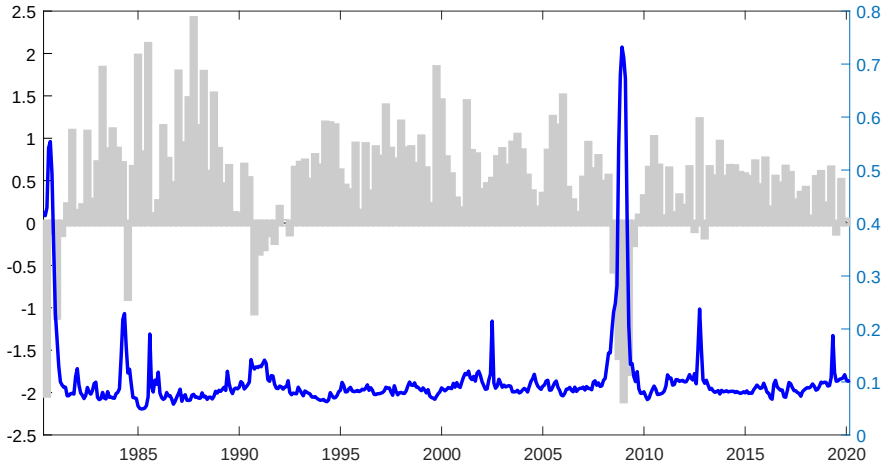

(b) Probability of low economic activity regime: Time-varying mean model

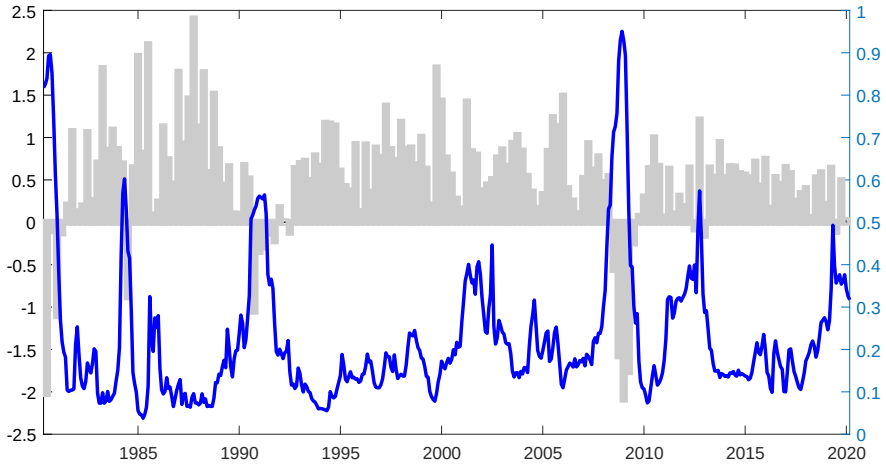

Note: The blue solid line (right axis) plots the monthly probability of low real activity regime, $Pr(s_t = 1)$, for the corresponding model, and the grey bars (left axis) denote the real GDP quarterly growth.

Figure 15: Brazil

(a) Probability of low economic activity regime: Constant mean model

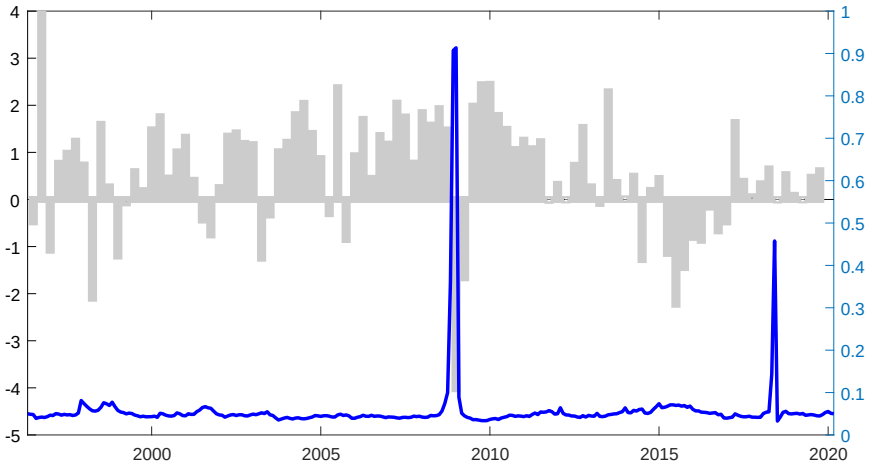

(b) Probability of low economic activity regime: Time-varying mean model

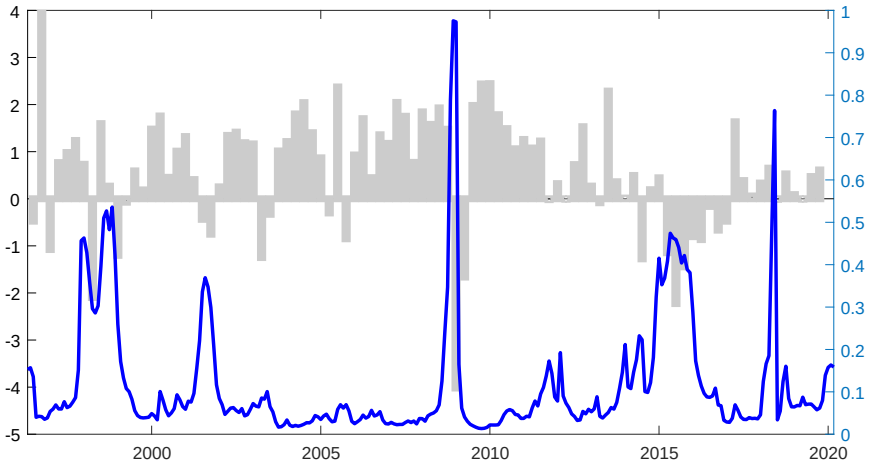

Note: The blue solid line (right axis) plots the monthly probability of low real activity regime, $Pr(s_t = 1)$, for the corresponding model, and the grey bars (left axis) denote the real GDP quarterly growth.

Figure 16: Mexico

(a) Probability of low economic activity regime: Constant mean model

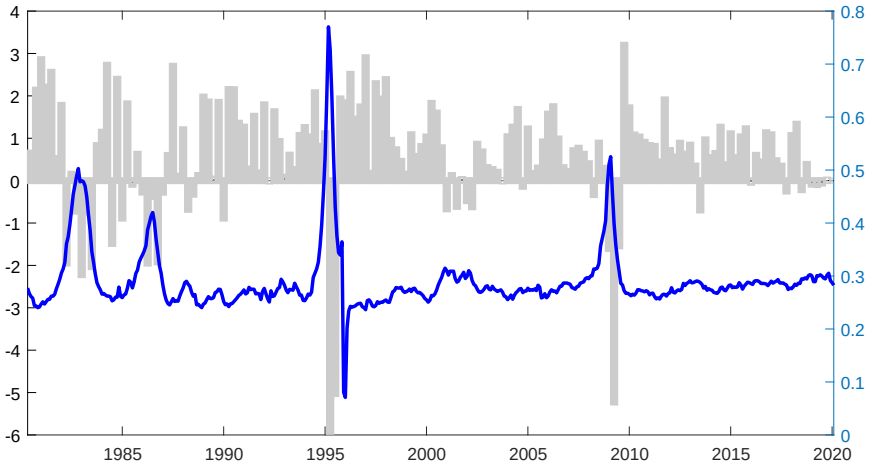

(b) Probability of low economic activity regime: Time-varying mean model

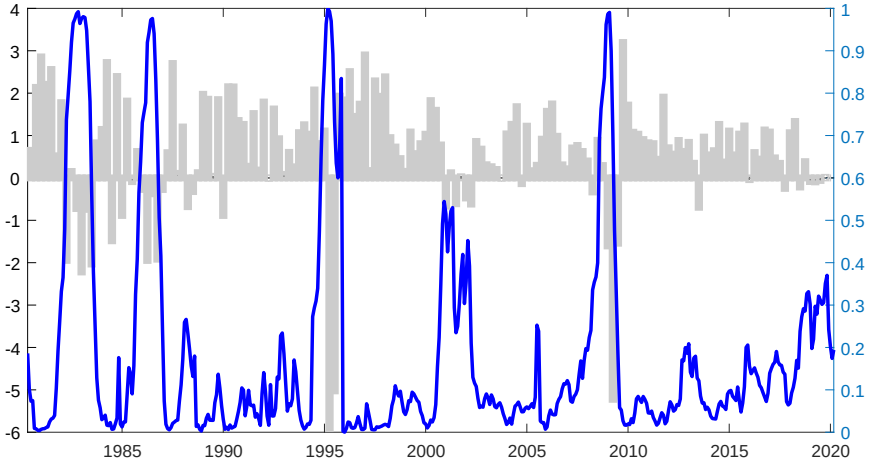

Note: The blue solid line (right axis) plots the monthly probability of low real activity regime, $Pr(s_t = 1)$, for the corresponding model, and the grey bars (left axis) denote the real GDP quarterly growth.

Figure 17: Russia

(a) Probability of low economic activity regime: Constant mean model

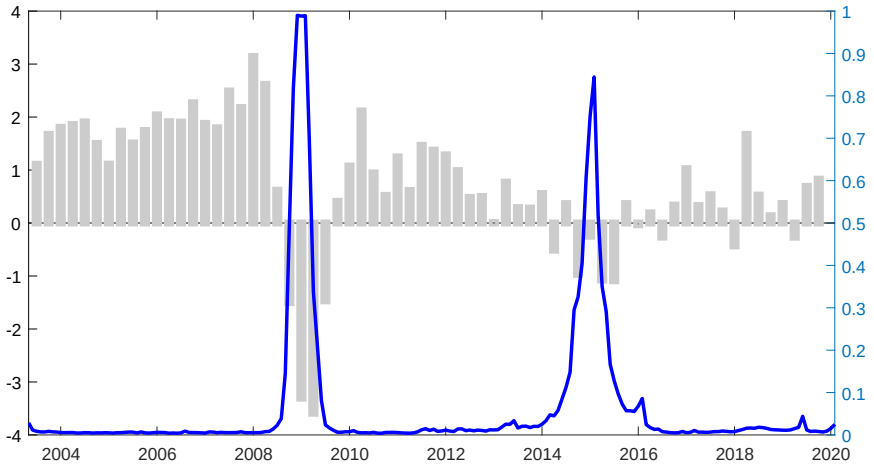

(b) Probability of low economic activity regime: Time-varying mean model

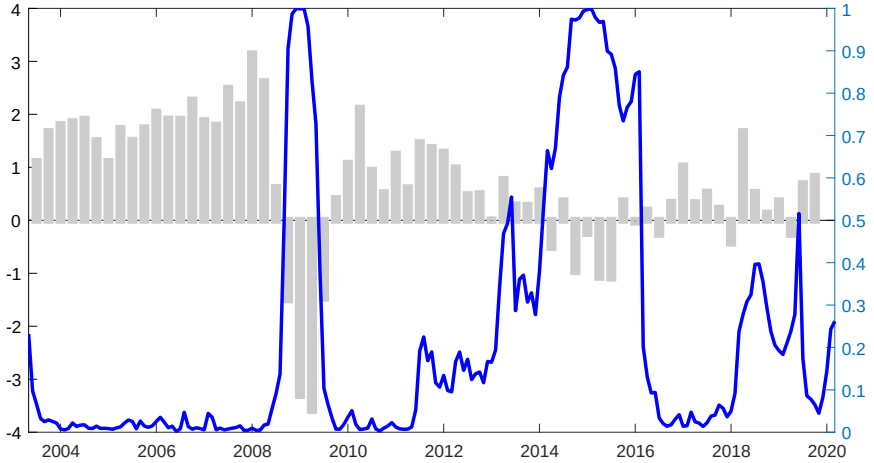

Note: The blue solid line (right axis) plots the monthly probability of low real activity regime, $Pr(s_t = 1)$, for the corresponding model, and the grey bars (left axis) denote the real GDP quarterly growth.

Figure 18: India

(a) Probability of low economic activity regime: Constant mean model

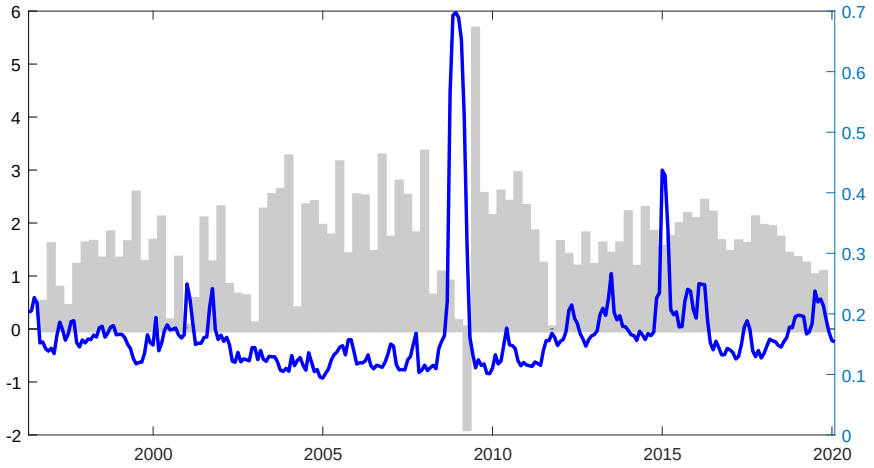

(b) Probability of low economic activity regime: Time-varying mean model

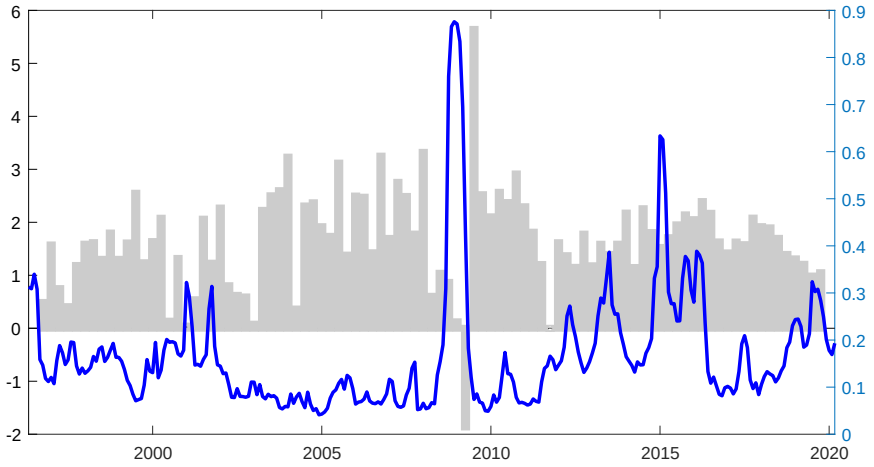

Note: The blue solid line (right axis) plots the monthly probability of low real activity regime, $Pr(s_t = 1)$, for the corresponding model, and the grey bars (left axis) denote the real GDP quarterly growth.

Figure 19: China

(a) Probability of low economic activity regime: Constant mean model

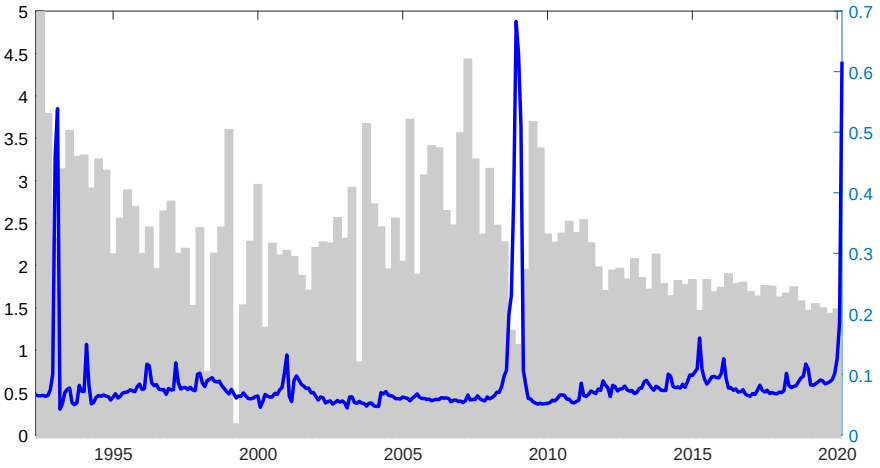

(b) Probability of low economic activity regime: Time-varying mean model

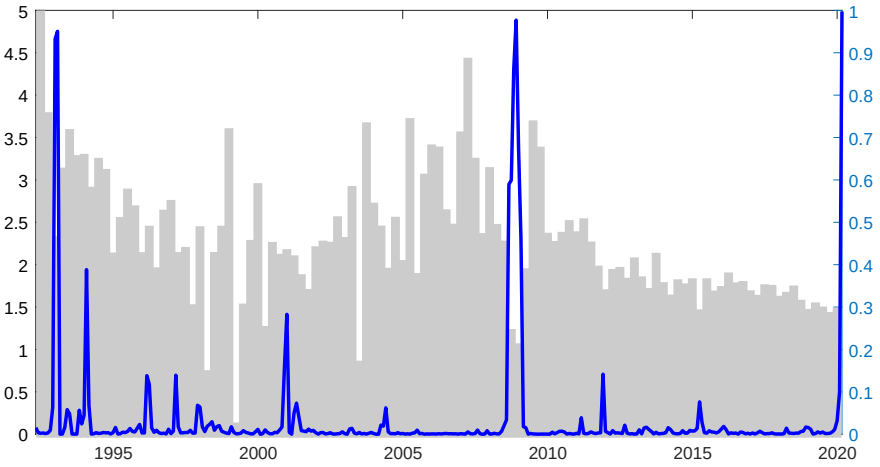

Note: The blue solid line (right axis) plots the monthly probability of low real activity regime, $Pr(s_t = 1)$, for the corresponding model, and the grey bars (left axis) denote the real GDP quarterly growth.

Figure 20: South Africa

(a) Probability of low economic activity regime: Constant mean model

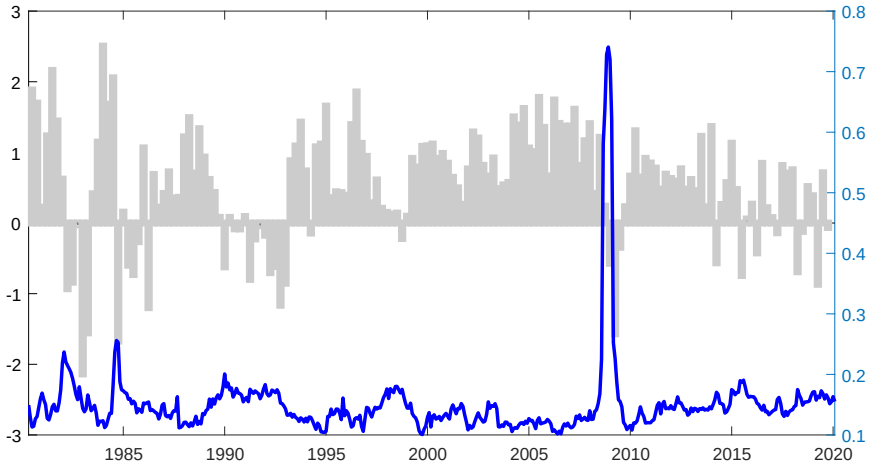

(b) Probability of low economic activity regime: Time-varying mean model

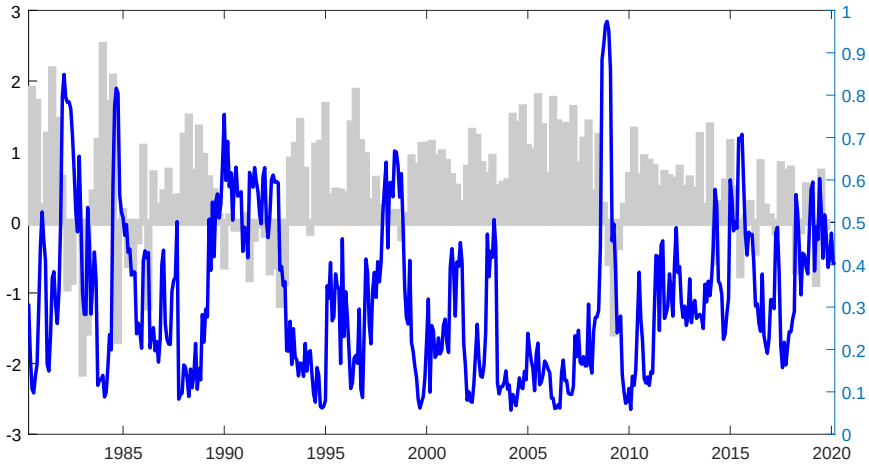

Note: The blue solid line (right axis) plots the monthly probability of low real activity regime, $Pr(s_t = 1)$, for the corresponding model, and the grey bars (left axis) denote the real GDP quarterly growth.

Figure 21: Time-varying component of mean growth during recessions

(a) U.S.

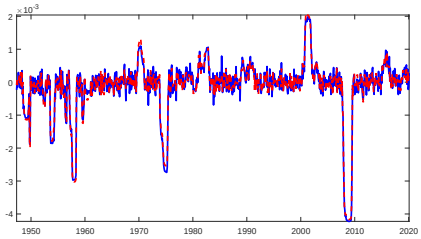

(b) Euro Area

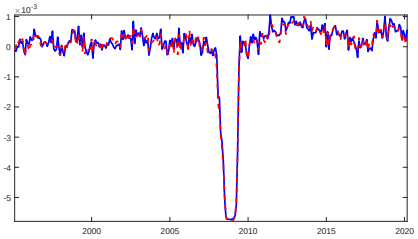

(c) United Kingdom

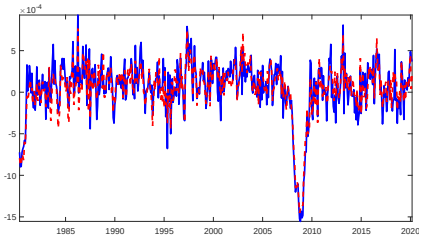

(d) Canada

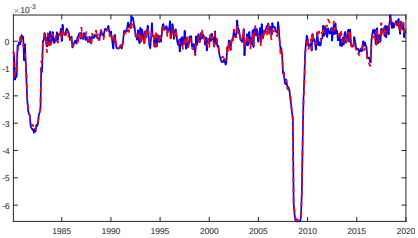

(e) Japan

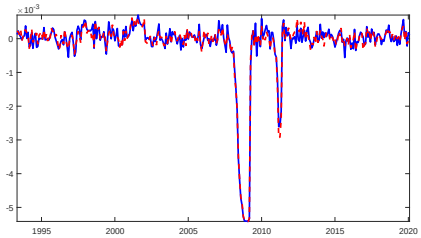

(f) Australia

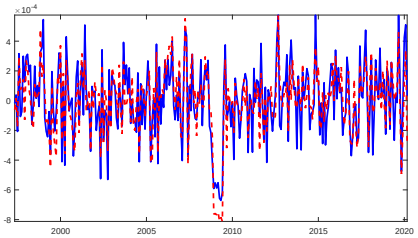

(g) Brazil

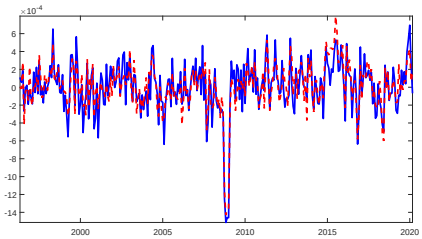

(h) Mexico

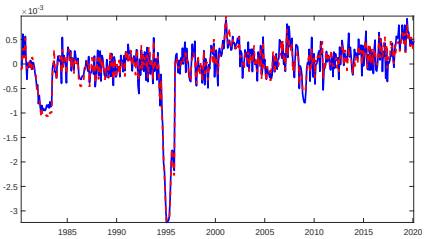

(i) Russia

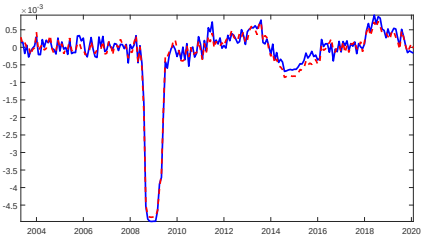

(j) India

(k) China

(l) South Africa

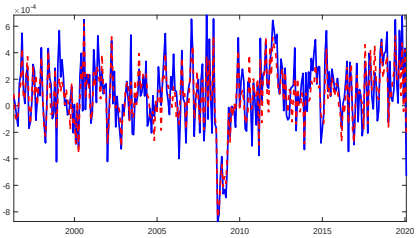

Note: The figure plots, for each country, the mean (solid blue line) and median (dashed red line) of the simulated distribution of the time-varying recession mean component, u_{τ_1}.

Acknowledgements

We would like to thank our colleagues of the ESCB Expert Group on Nonlinear Models for their stimulating and helpful comments. The views expressed in this paper are those of the authors and are in no way the responsibility of the Banco de España, European Central Bank, Eurosystem, or Magyar Nemzeti Bank.

Danilo Leiva-Leon
Banco de España, Madrid, Spain; email: danilo.leiva@bde.es

Gabriel Perez-Quiros
European Central Bank, Frankfurt am Main, Germany; CEPR; email: gabriel.perez_quiros@ecb.europa.eu

Eyno Rots
Magyar Nemzeti Bank, Budapest, Hungary; email: rotse@mnb.hu

Postal address 60640 Frankfurt am Main, Germany
Telephone +49 69 1344 0
Website www.ecb.europa.eu

PDF ISBN 978-92-899-4024-5 ISSN 1725-2806 doi:10.2866/24670 QB-AR-20-033-EN-N